AN ALTERNATIVE METHOD TO DESIGN POST-FRAME BUILDINGS WITHOUT TESTING ROOF DIAPHRAGM

A Thesis

Presented to the Faculty of the Graduate School

of Cornell University

In Partial Fulfillment of the Requirements for the Degree of

Master of Science

by

Shule Hou

August 2016

ABSTRACT

The current diaphragm design procedure for post-frame buildings is outlined in ANSI/ASAE Engineering Practice (EP) 484.2 (2012) *Diaphragm Design of Metal-clad, Post-Frame Rectangular Buildings*. According to ANSI/ASAE EP484.2 (2012), the stiffness of metal-clad wood-frame (MCWF) diaphragm must be known for proper analysis and design of the post-frame buildings. A database of stiffness of MCWF diaphragm is lacking in literature. These design values are typically derived through small-scale panel tests. However, this test method is costly and requires considerable time to perform the test.

The contribution of this research is to create an alternative method (Allowable Eave Deflection (AED) method) to design post-frame buildings without testing the whole MCWF diaphragm. The AED method utilizes the model of the current research (Modified MCA procedure) to build relationship between the stiffness of the MCWF diaphragm and horizontal eave deflection. The stiffness of the MCWF diaphragm is obtained based on the defined maximum horizontal eave deflection.

BIOGRAPHICAL SKETCH

Shule Hou was born in August 20, 1991 in Beijing, China. He received the Bachelor of Engineering in Department of Civil Engineering at Beijing University of Civil Engineering and Architecture. Then, he studied under the guidance of Professor Kifle G. Gebremedhin in School of Civil and Environmental Engineering at Cornell University. His research includes construction of three-dimensional stiffness model of metal-clad post-frame buildings, structural analysis of post-frame buildings with diaphragm action, and estimation of the stiffness of roof diaphragm.

ACKNOWLEDGEMENTS

I would like to thank Professor Kifle G. Gebremedhin, Professor Kenneth Hover for agreeing to serve as my advisory committee. I would particularly like to thank my advisor Professor Kifle G. Gebremedhin for his guidance and assistance during my thesis research. I would also like to thank my committee member Professor Kenneth Hover for their assistance and suggestions throughout the last two years.

I am greatly indebted to my friends at Cornell who have provided tremendous support and invaluable suggestions during the preparation of my thesis. Especially thank for Haoran and Jiajun for their encouragement and support during thesis defense.

Last but not least, I would like to thank my parents, Baozhong and Xuyi, for their unconditional support, encouragement and love, without which I would not have come this far.

TABLE OF CONTENTS

CHAPTER 1: INTRODUCTION

The history of the post-frame building can be traced back to pole building on 17th century (Figure 1). The post-frame building system is similar to pole building systems. This system is characterized by primary structural frames of wood posts as columns and rafters as roof framing. Roof framing is attached to the wood posts. Wood posts are embedded in the soil. Secondary framing members (purlins in the roof and girts in the walls) are used to provide lateral support and transfer load to the roof framing and wood posts. Figure 2 illustrates the various components of a typical post-frame building.

Figure 1 Frame of pole building barrack erected in 2011 in effort to duplicate construction methods used during the colonization of Jamestown. (NFBA Post-frame Building Design Manual, 2015)

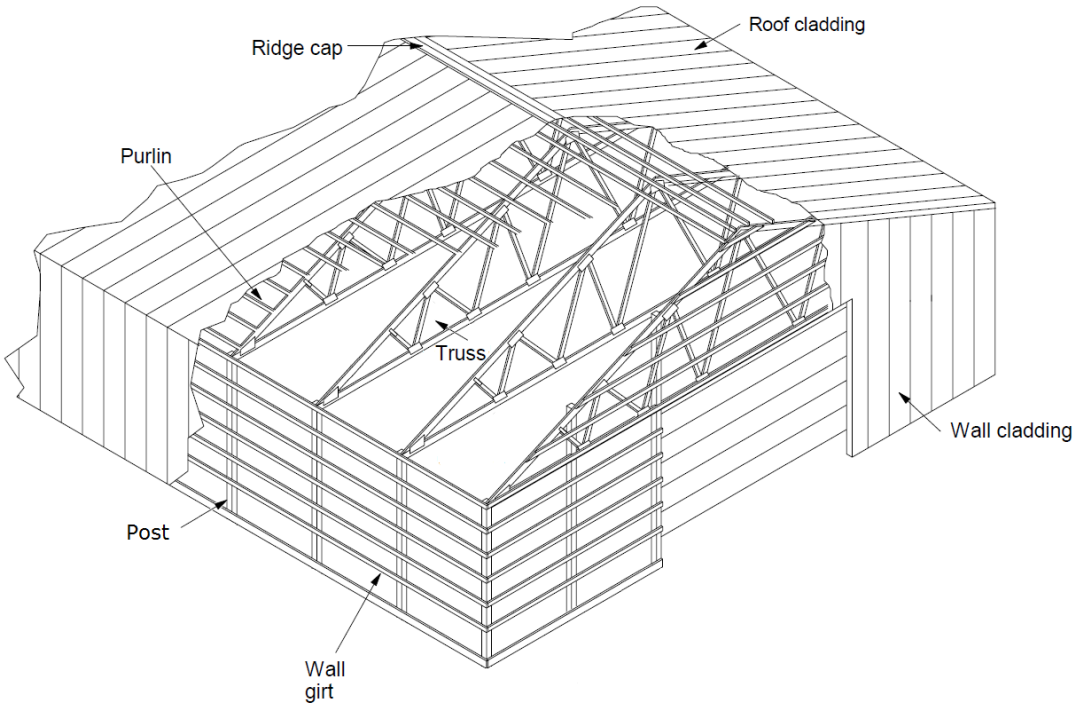

Figure 2. Components of a typical post-frame building (Post-frame Building Design Manual,1999)

For centuries, post-frame buildings have been the subject of considerable research aimed at designing post-frame building properly. There are two common design methods for post-frame buildings: two dimensional (2-D) “stick” frame design method and diaphragm design method. In 2-D “stick” frame design method, the structure is considered as a system of independently-acting, 2-D post-frames. Although the 2-D frame design method works well for frames under vertical loadings; it is often too conservation to design post-frame buildings against sidesway without considering diaphragm action (NFBA Post-Frame Building Design Manual, 2015). Diaphragm action is transfer of in-plane loads (wind and seismic) to end walls via cladding by shear. Diaphragm design method is to design a post-frame building considering diaphragm action.

Applying the principle of diaphragm action results in reduced post size and embedment requirement consistent with actual building performance (NFBA Post-Frame Building Design Manual, 2015). For example, the post is reduced from an 8-by-8 solid-sawn (or 4-ply, 2-by-8 laminated) column when no diaphragm action is used, to a 6-by-6 solid-sawn (or 3-ply, 2-by-6 laminated) column when diaphragm action is considered for a 40ft wide by 80ft long building (Post-Frame Construction Guide, 2000). The cost reduces about $30 per post (Midwest Perma-Column website), which is the benefit of utilizing diaphragm design.

Current diaphragm design procedure is outlined in ANSI/ASAE Engineering Practice (EP) 484.2 (2012) *Diaphragm Design of Metal-clad, Post-Frame Rectangular Buildings*. The most important step of the ANSI/ASAE EP484.2 method is to determine the horizontal load distribution to frames and metal-clad wood-frame (MCWF) diaphragm (typically roof diaphragm and endwall diaphragm). This load distribution can be calculated after the stiffness values are known for each frame and the MCWF diaphragm. Currently, the most common method to obtain the stiffness of the MCWF diaphragm is by testing a small-scale diaphragm. Although most common design values obtained from small-scale tests are limited because of their cost and considerable time required to perform tests (Aguilera, 2014). Currently, database for stiffness of MCWF diaphragms is lacking in the literature. In the NFBA Post-Frame Building Design Manual (2015), there are only 19 MCWF roof diaphragm test data and 5 MCWF endwall test data. If there is any change in the construction of the MCWF diaphragm such as wood species, wood grade, fastener size, fastener spacing, etc., a new stiffness of MCWF diaphragm

must be determined by conducting a new test. Therefore, an alternative method is required to predict stiffness of MCWF diaphragm placing less or no reliance on test.

This study presents a mathematical method to predict stiffness of metal-clad wood-frame (MCWF) diaphragm called Allowable Eave Deflection (AED) method. The AED method is an extension of the current work on the modified MCA procedure. The modified MCA procedure utilizes the stiffness of purlin-rafter connection to predict the stiffness of roof diaphragm. The stiffness of purlin-rafter connection is obtained by the test procedure develped by Leflar (2008). The test procedure for purlin-rafter connection is much easier and cheaper than the small-scale test for the whole MCWF diaphragm. Although the modified MCA procedure provides an accurate prediction of the stiffness of the MCWF diaphragm, the time investment to learn the procedure and its complexity are significant barriers to implement (Aguilera, 2014). The AED method utilizes the modified MCA procedure to establish the relationship between the stiffness of a MCWF diaphragm and horizontal eave deflection for the critical frame. The stiffness of the MCWF diaphragm can be directly calculated by the AED method without understanding the modified MCA procedure.

CHAPTER 2: LITERATURE REVIEW

This chapter contains four parts. Section 2.1 describes the behavior of post-frame building considering diaphragm action. Section 2.2 presents the development of design procedure for post-frame buildings. Section 2.3 shows the current study on metal-clad wood-frame diaphragm. Section 2.4 provides a summary of computer programs available for analyzing and design of post-frame buildings.

2.1 Behavior of post-frame building considering diaphragm action

The behavior of post-frame building considering diaphragm action can be investigated using a full-size test of a post-frame building. Two primary purposes of the full-scale building tests were to demonstrate the contribution of steel cladding to building stiffness, and to determine load distribution in a post-frame building (Bohnhoff, 2002). Several researchers have performed full-size test of post-frame buildings (Johnston and Curtis (1984), McFadden et al. (1991), Gebremedhin et al. (1992)). One of the main researches conducted to understand load distribution in a post-frame building is the full-size building test conducted at Cornell by Gebremedhin et al. (1992).

Gebremedhin et al. (1992) constructed a full-size post-frame building and tested it in six stages of construction to determine the contribution of each component to the stiffness of the building. The building used in the test was 40-ft wide by 80-ft long by 16.25-ft to the eave height. The post-truss frames were spaced 8-ft on center, and the roof slope was 4:12. Wind loading was simulated by applying concentrated loads of equal magnitude at each of the

interior post-frames on the structure at different stages of construction. These construction stages consisted of:

(1) Wood framing with no steel sheathing;

(2) Steel sheathing attached to the endwalls only;

(3) Steel sheathing attached to the endwalls and sideswalls;

(4) Steel sheathing attached to all walls and one side of the roof;

(5) Steel sheathing attached to all walls and both sides of the roof with the ridge cap also fastened;

(6) With the ridge cap fasteners removed from one side of the roof.

The first test showed eave deflection at the middle frame was equal to 6.1-in. The second and third test illustrated the cladding of the walls made little contribution to the stiffness of the whole building. From the fourth and fifth test, eave deflection at the middle frame was reduced from 6.1in (155mm) to 0.44in (12mm), a 93% reduction. The final test is to see whether the ridge cap transfers shear from one side of the roof to the other side of the roof. The result showed that if the ridge cap is fastened properly, shear is transfer from one side of the roof to the other side.

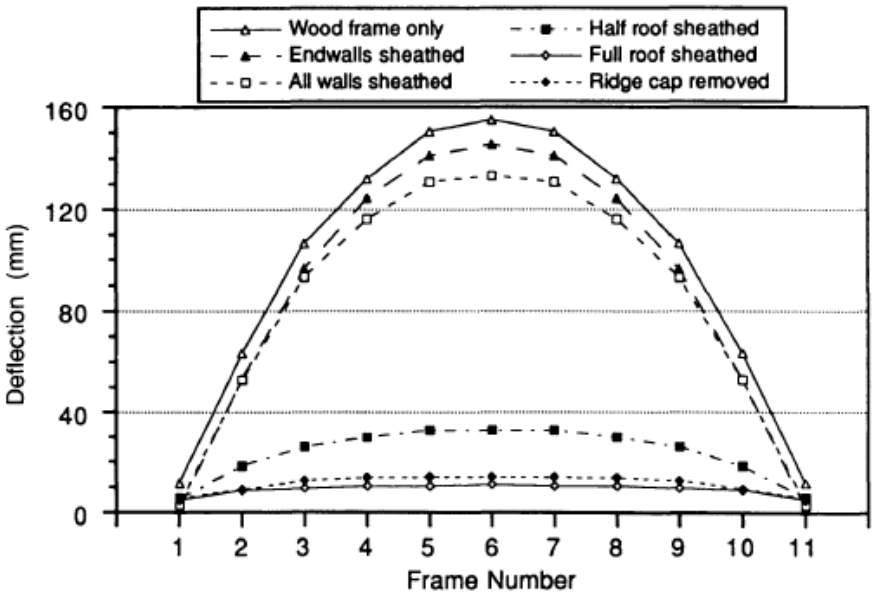

Figure 3 Measured eave deflections of all test stages when 425lb concentrated force was applied at each interior post-frame (Gebremedhin et al. 1992)

Niu and Gebremedhin (1997a) tested the same full-scale post-frame building, but the loading was different. A single lateral eave load was applied at eave height of each post-frame one-at-a-time and eave displacements were measured of all frames (Figure 4). The purpose of this loading case was to evaluate the actual physical symmetry, and to illustrate the load sharing among frames as the loading shifts from one frame to another (Niu and Gebremedhin, 1997a).

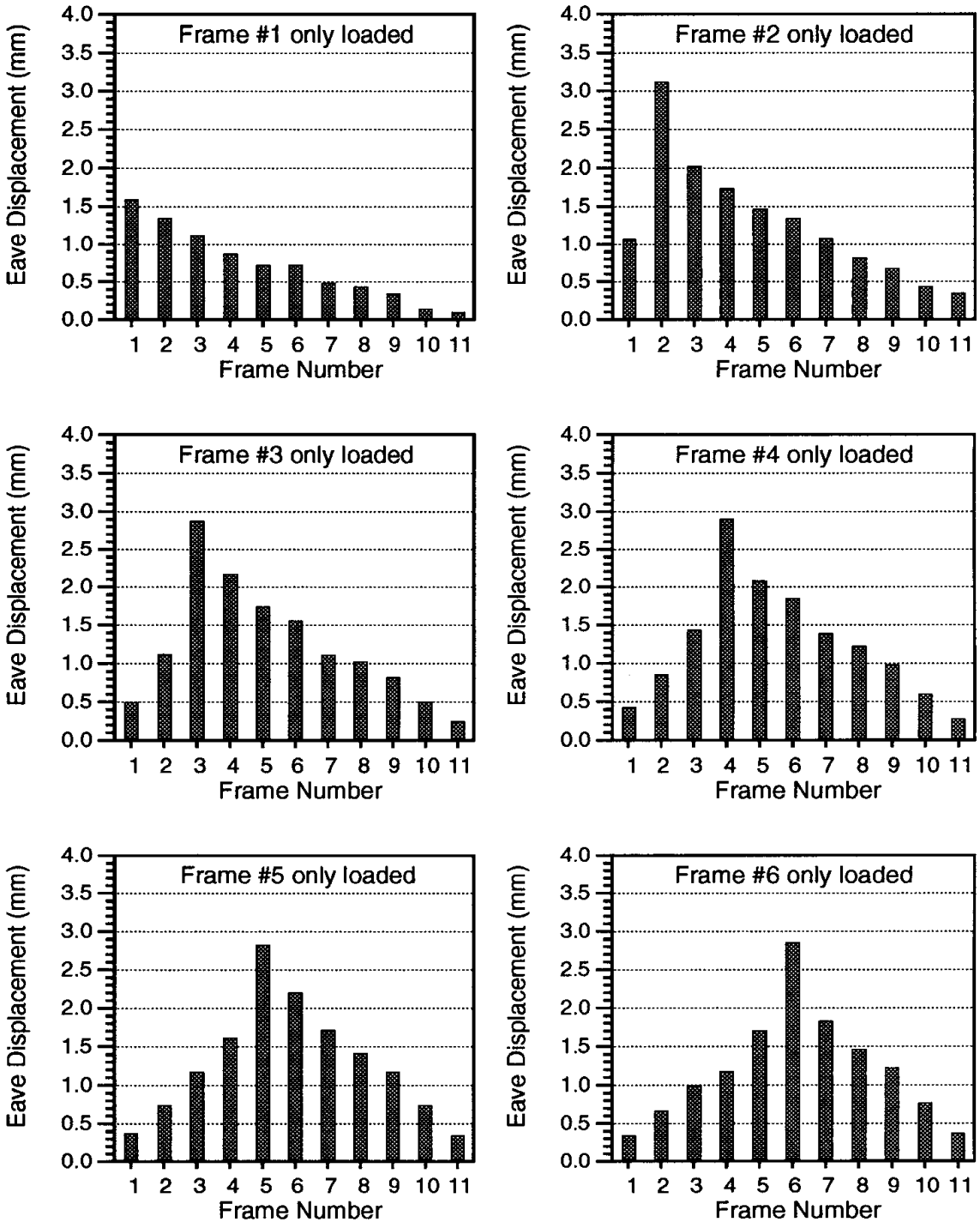

Figure 4a Eave displacement profile when an eave load of 1000lb was applied at each frame (Niu and Gebremedhin, 1997a)

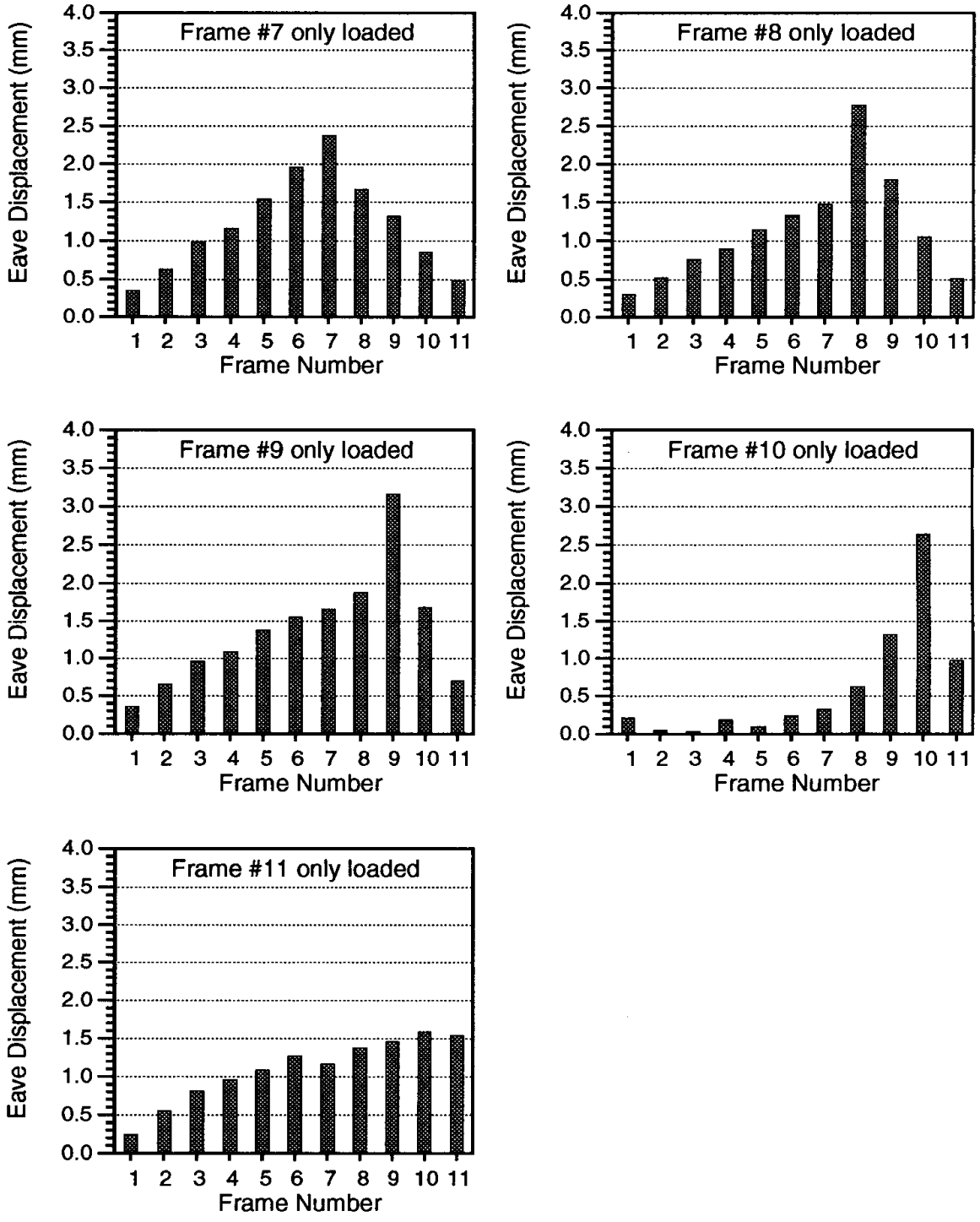

Figure 4b Eave displacement profile when an eave load of 1000lb was applied at each frame (Niu and Gebremedhin, 1997a)

While it is impractical to conduct a full-size test for every post-frame building due to the high cost of equipment and material, the full-size test data provided important information about the behavior of post-frame building considering diaphragm action.

2.2 Design procedures of post-frame buildings

Experimental research has been done to investigate the behavior of post-frame building considering diaphragm action. In the past couple decades, a great deal of research has been done to analyze and design post-frame building considering diaphragm action.

Hoagland and Bundy (1983) developed a procedure for designing metal-clad wood-frame (MCWF) building including diaphragm action. This design procedure required in-plane strength and stiffness data for the roof diaphragm. The data of in-plane strength and stiffness were obtained from Hoagland and Bundy (1983) *Strength and Stiffness of Screw-Fastened Roof Panels for Pole Buildings*. Hoagland and Bundy (1983) also recommended using a computer program for analyzing 2-dimensional frames. A summary of the computer program used for designing a post-frame building is shown in Section 2.4.

Gebremedhin et al. (1986) modified the procedure by Hoagland and Bundy (1983) by creating design tables for the resistance force to sidesway modifiers (mD) and shear force in the roof cladding modifier (mS). Design Tables for modifiers (mD) and (mS) due to diaphragm action are derived for buildings up to 30 frames. Gebremedhin et al. (1986) also recommended that the roof diaphragm sidesway resistance force, Q, be distributed as a horizontal uniform load, q, along the top chords of the truss (Figure 5). This treatment replaces application of a single concentrated resistance force to sidwsway at eave height (Hoagland and Bundy, 1983).

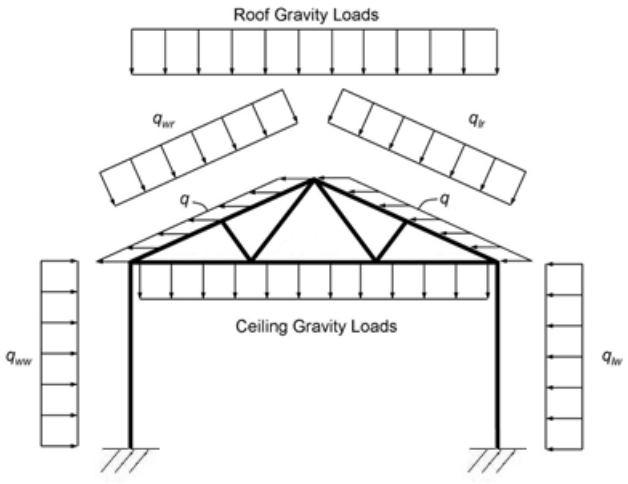

Figure 5 Structural analog for a building with roof diaphragms resisting force, q (ASAE EP484, 1989)

The first version of ASAE Engineering Practice (EP) 484 *Diaphragm Design of Metal-clad, Post-Frame Rectangular Buildings* was approved for publication in 1989. ASAE EP484 (1989) diaphragm design procedures are based on the methods developed by Gebremedhin et al. (1986). This Engineering Practice also standardizes the methods for laboratory testing and reporting the strength and stiffness of metal-clad, wood-frame diaphragms.

Anderson et al. (1989) developed the "force distribution" method to determine load distribution between building frames and roof diaphragm. This method is an iterative longhand method for the analysis of post-frame buildings and does not require the solution of simultaneous equations. A two-dimensional spring model with frame and diaphragm element stiffness values and individual point loads at the eave are shown in Figure 6. This method allows analyzing frames that have different stiffness values, end walls that may be flexible and point loads at the eave that may have different values.

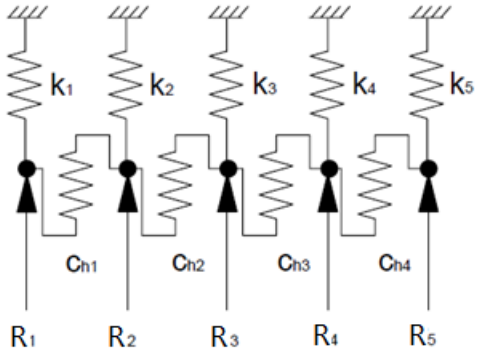

Figure 6 Two-dimensional spring model (NFBA Post-Frame Building Design Manual, 2015)

where,

k_i = stiffness of frame i

C_{hi} = stiffness of roof diaphragm i

Ri = eave load at frame i

Niu and Gebremedhin (1997b) developed a 3-dimensional model (Figure 7) for the purposes of extrapolating laboratory-test panel stiffness data to full-scale diaphragm, predicting building eave displacement and determining upper-bound post-frame building strength. Model predictions were compared to full-scale building test data (Gebremedhin et al., 1992), and eave deflection prediction error ranged between 2% and 17%.

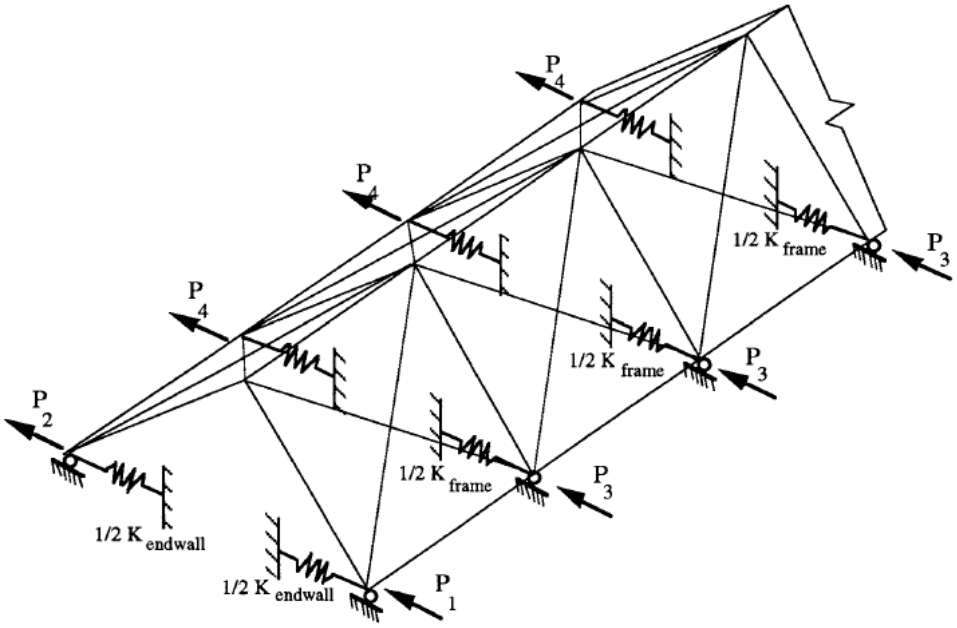

Figure 7 A three-dimensional structural analog of the post-frame building (Niu and Gebremedhin, 1997b)

In 1998, a major version to the ASAE EP484 was completed (ASAE EP484.2, 1998). This reversion allowed for more detailed diaphragm analyses including the force distribution method developed by Anderson (1989) and computer program DAFI developed by Bohnhooff (1992). The ASAE EP484 (1989) covering diaphragm panel tests were removed from the standard and placed in a separate publication titled ASAE EP558 *Load Tests for Metal-Clad Wood-Frame Diaphragms.* In August 1998, the ASAE EP484.2 was approved by ANSI as an American National Standard. The ANSI/ASAE EP484.2 (2012) is the most up-to-date document on design of post-frame structures utilizing diaphragm action (NFBA Post-Frame Building Design Manual, 2015).

Applying the principles of diaphragm action results in reduced post size and embedment requirement consistent with actual building performance (NFBA Post-Frame Building Design Manual, 2015). According to the ANSI/ASAE EP484.2 (2012), stiffness values for each frame and

metal-clad wood-frame (MCWF) diaphragm (typically roof diaphragm and endwall diaphragm) must be known to determine the horizontal load distribution to frames and MCWF diaphragm. However, currently the database of stiffness of MCWF diaphragm is lacking in the literature.

2.3 Current study on metal-clad wood-frame diaphragm

Currently, the most common method to obtain the stiffness of the MCWF diaphragm is through a small-scale diaphragm test. Design values from small-scale tests are limited because of their cost and considerable time required to perform the tests (Aguilera, 2014). Leflar (2008) and Anderson (2011) developed a model to predict strength and stiffness of metal-clad wood-framed diaphragms. This model, referred to as the modified MCA procedure, allows design strength and stiffness values to be predicted analytically with less reliance on expensive diaphragm testing (Anderson, 2011).

The MCA procedure is a mathematical method for determining strength and stiffness for metal-clad steel-framed diaphragms. The MCA procedure was developed by Luttrell and Mattingly (2004) and published by the Metal Construction Association. The MCA procedure has been widely used by the steel industry.

Leflar (2008) and Anderson (2011) modified the MCA procedure by adding the total out-of-plane rafter-purlin connection stiffness, K_R, to the in-plane stiffness of metal cladding to determine the stiffness of metal-clad wood-frame (MCWF) diaphragm. A spring analog of loads through rafter-purlin connections and metal cladding is shown in Figure 8.

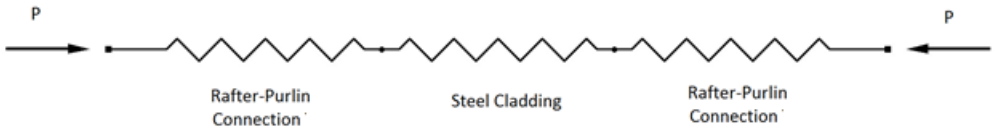

Figure 8. A spring analog of loads through rafters and MCWF diaphragm (Leflar, 2008)

The total rafter-purlin connection stiffness for a single rafter, K_R, is the sum of all of the rafter-purlin stiffness values, K_p, plus the sum of all the shear-block stiffness values on the rafter, K_{sb}. A typical shear block used in diaphragm construction is shown in Figure 9. A spring analog of a rafter-purlin connections is shown in Figure 10.

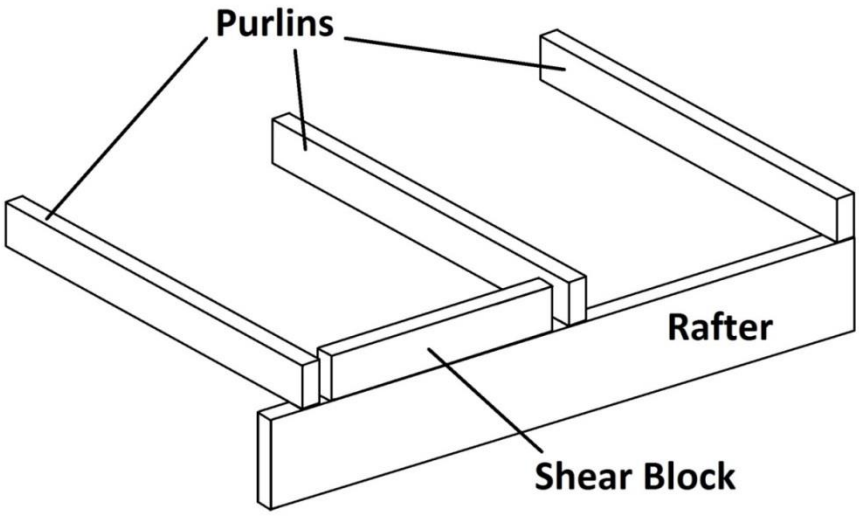

Figure 9. A typical shear-block used in diaphragm construction to increase strength and stiffness

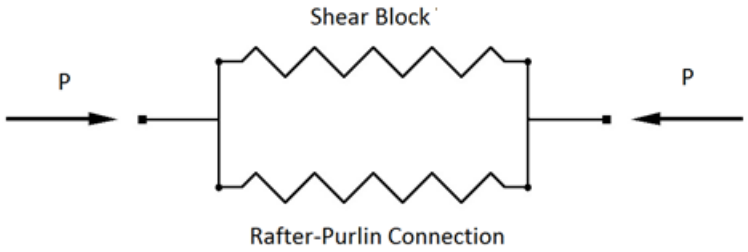

Figure 10. A spring analog of rafter-purlin connections

Leflar (2008) tested rafter-purlin connections and rafter-shear block connection to determine stiffness. The results are shown in Table 1. If purlins or blocking of different size, connection type, or significantly different specific gravity of wood are used, the connection stiffness must be determined by testing using similar methods established by Leflar (2008).

Table 1. Strength and stiffness of rafter-purlin and rafter-shear block connection (Leflar 2008)

Member	Connection	Size	Orientation	Location	Specific Gravity	Stiffness (kips/ft)
Rafter-Purlin connection	1-60d hardened steel ring shank nail	2*4	on-edge	on top of rafter	0.42	1.0
Rafter-shear block connection	2-60d hardened steel ring shank nail	2*4	on-edge	on top of rafter	0.42	10.0

Leflar (2008) also tested 26 different diaphragm constructions in accordance with ASAE EP-558(2014). The modified MCA procedure predicts an average strength of 98% of test diaphragm strength and an average stiffness of 97% of test diaphragm stiffness. The coefficient of variability of 16% for strength and 23% for stiffness are within the variability of a single species and grade of wood as specified by the National Design Standard (NDS) (Leflar, 2008).

Aguilera (2014) developed design tables to determine the in-plane shear modulus of a metal-clad wood-frame diaphragm of common constructions shown in Table 2. The modified

MCA procedure is being considered for the next reversion of the ANSI/ASAE EP484.2 diaphragm design standard (Aguilera, 2014).

Table 2. Design values governed by screws for 9 in. major rib spacing (Aguilera 2014)

Purlin Spacing = 2 ft. Minimum Purlin S.G. = 0.42 Major Rib Bottom Width Range = 1 - 2.5 in. Major Rib Spacing = 9 in. Major Rib Height Range = 0.625 - 1.0 in. Major Rib Top Width Range = 0.25 - 0.75 in.							
Min. Yield/Ultimate Strength	Gauge	Field Screws into Flats	Screws into Panel Overlap	For No Screws into Panel Overlaps	Spacing of screws into the panel overlaps (in.)		
					24	12	8
				G'	G'	G'	G'
(ksi)				(kips/in)	(kips/in)	(kips/in)	(kips/in)
80/82	28 (.0149")	#9-1"	None	2.8	-	-	-
			#10 Stitch	-	19	27	32
			#12 Stitch	-	19	27	32
		#10-1"	None	2.8	-	-	-
			#10 Stitch	-	19	27	32
			#12 Stitch	-	19	27	32
		#10-1.5"	None	2.8	-	-	-
			#10 Stitch	-	19	27	32
			#12 Stitch	-	19	27	32
		#12-1.5"	None	2.8	-	-	-
			#10 Stitch	-	19	27	32
			#12 Stitch	-	19	27	32
	29 (.0135")	#9-1"	None	2.8	-	-	-
			#10 Stitch	-	18	25	29
			#12 Stitch	-	18	25	29
		#10-1"	None	2.8	-	-	-
			#10 Stitch	-	18	25	29
			#12 Stitch	-	18	25	29
		#10-1.5"	None	2.8	-	-	-
			#10 Stitch	-	18	25	29
			#12 Stitch	-	18	25	29
		#12-1.5"	None	2.8	-	-	-
			#10 Stitch	-	18	25	29
			#12 Stitch	-	18	25	29

2.4 Computer program for analyzing and designing post-frame buildings

Analyzing post-frame buildings including diaphragm action is best performed with a computer program. Several computer programs have been developed for analyzing and designing post-frame buildings.

Gebremedhin (1987) developed a computer program called SOLVER for analyzing two or three dimensional skeletal structures such as continuous beams, trusses, and frames. SOLVER can analyze structures with uniform or non-uniform cross sections and with either pinned or rigid connections. In order to use SOLVER in diaphragm design, we have to run it three times. The first run is to calculate the frame stiffness; the second run is to determine the eave load; the last run is to analysis the member forces and moments with diaphragm resisting force. SOLVER required the stiffness of roof diaphragm to account for diaphragm action.

Gebremedhin (1988) developed a computer program called METCLAD for use in diaphragm analysis and design of metal-clad post-frame rectangular buildings. METCLAD combined all of the procedures required to perform diaphragm design so that no initial or intermediate calculations are performed by the user. METCLAD provided results including structural responses of the building such as member forces, moments and deflections, node displacements, support reactions, shear analyses, combined stress interaction analyses and location of maximum stresses of members. METCLAD also requires the stiffness of roof diaphragm to account for diaphragm action.

Bohnhoff (1992b) wrote a computer program, DAFI (Diaphragm and Frame Interaction), for the purpose of determining load distribution of the individual frames and diaphragms. DAFI

eliminates the rigorous manual calculation associated with the “force distribution” method and can be used to analyze buildings in which bay spacings vary, the stiffness of individual frames differ, endwalls are not assumed infinitely rigid, and/or the stiffness of individual diaphragms are not the same (Bohnhoff, 1992b). DAFI requires the stiffness of roof diaphragm and stiffness of endwall.

The Purdue Plane Structures Analyzer 4 (PPSA4) is a two-dimensional structural analysis and design program written specifically for use in designing wood components and structures (Triche and Suddarth, 1993). PPSA4 can be used to analyze and design most commercially available wood products including solid sawn, glulam, etc. This computer program is similar to SOLVER that we have to run iy three times to design building considering diaphragm action. PPSA4 also required the stiffness of roof diaphragm and stiffness of endwall.

In the new version of NFBA Post-Frame Building Design Manual (2015), only computer program DAFI is recommended to determine the load distribution due to diaphragm action. However, DAFI is not a computer program written for design. The designers have to do hand calculations to design wood post.

CHAPTER 3: METHODOLOGY

In this chapter, the Allowable Eave Deflection (AED) method is presented as an alternative method to predict the stiffness of the metal-clad wood-frame (MCWF) diaphragms without a small-scale test. The general procedure of the AED method can be broken down into six steps:

Step 1: Calculation of frame stiffness (Section 3.1) and eave loads (Section 3.2)

Step 2: Selection of in-plane diaphragm stiffness modulus (Section 3.3) from the database (Aguilera, 2014).

Step 3: Calculation of stiffness of roof diaphragm (Section 3.4) and stiffness of endwall (Section 3.5) in terms of in-plane diaphragm stiffness modulus for metal cladding.

Step 4: Calculation of diaphragm resistance force modifier (Section 3.6) and maximum horizontal eave deflection (Section 3.7)

Step 5: Based on the Monte Carlo Simulation, the in-plane diaphragm stiffness modulus for metal cladding is set as a variable to calculate stiffness of roof diaphragm, stiffness of endwall and maximum horizontal eave deflection.

Step 6: Based on the simulation data (stiffness of roof diaphragm, stiffness of endwall and maximum horizontal eave deflection) from Step 5, find best-fit line for stiffness versus maximum horizontal eave deflection curve.

The assumptions in the Allowable Eave Deflection (AED) method are: 1) Stiffness values of both endwalls are the same, 2) stiffness values of the interior frames are the same, 3)

stiffness values of the diaphragms of both slopes of the roof are the same, 4) eave loads for all interior frames are the same, 5) eave load for the exterior frame is equal to one-half that of the interior frame.

3.1 Frame stiffness, k

Frame stiffness, k, is generally obtained using a plane-frame structural analysis computer program. A horizontal force, P, applied at the eave height of a frame will result in a horizontal displacement of the eave, Δ, as shown in Figure 11. The ratio of the force, P, to the horizontal displacement, Δ, is defined as the horizontal frame stiffness which can be expressed as

$$k = P / \Delta \quad (1)$$

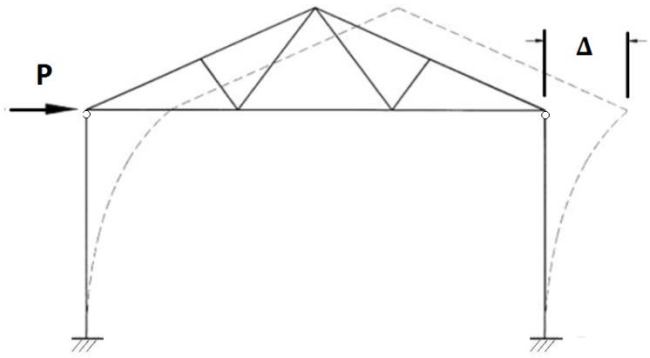

Figure 11 Definition sketch for frame stiffness, k (ANSI/ASAE EP484.2, 2012)

3.2 Eave load, R

Eave load is defined as an equivalent horizontally concentrated load that represents applied building loads for diaphragm design. The eave load and the applied building loads are equivalent in terms of the horizontal displacements at the eave height (Figure 12 & 13).

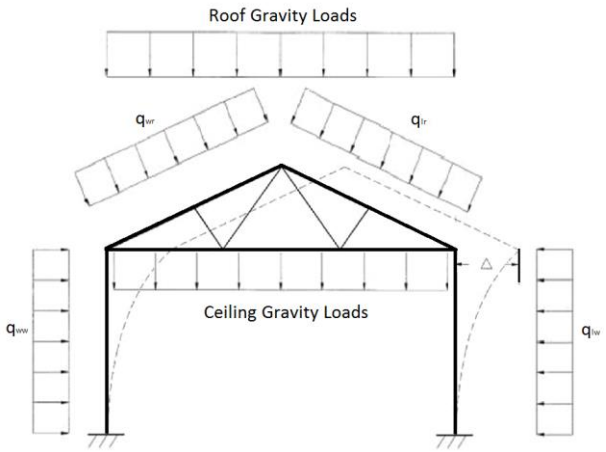

Figure 12 Eave deflection Δ due to all building loads

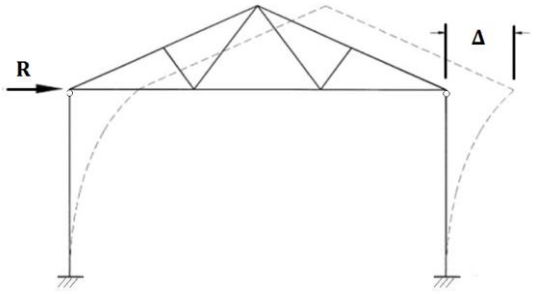

Figure 13 Identical deflection Δ due to eave load

To determine eave load, R, by a plane-frame structural analysis, a horizontal restraint (vertical roller) is placed at the eave line opposite to the direction of the load as shown in Figure 14. The horizontal reaction at the vertical roller support is numerically equal to the eave load, R.

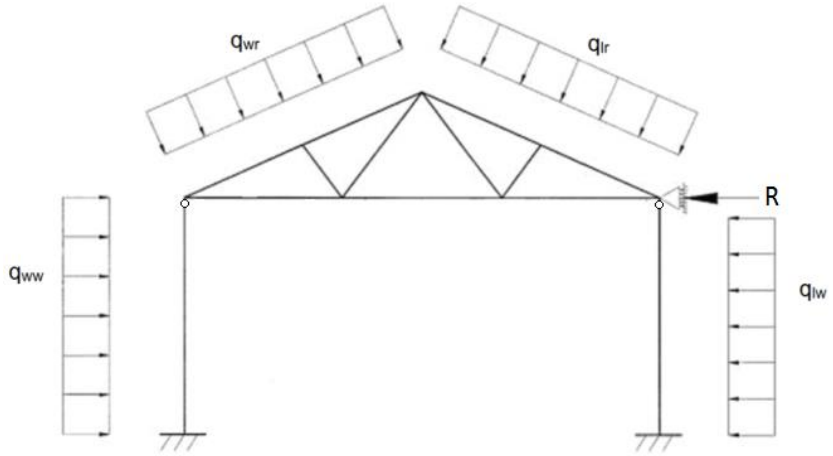

Figure 14 Structural analog for obtaining eave load, R (ANSI/ASAE EP-484.2)

3.3 The in-plane stiffness modulus for metal cladding

The in-plane stiffness modulus for metal cladding, G_{MCA}, is a constant value for a diaphragm with a given steel gauge thickness and stitch screw spacing (Aguilera, 2014). The database of Aguilera's test (2014) is given in Table 3.

Table 3. Comparison of minimum and maximum calculated in-plane stiffness (Aguilera, 2014)

Major Rib Spacing (in.)	Gauge	Stitch Screw Spacing (in.)	Minimum In-Plane stiffness (kips/in)	Maximum In-Plane Stiffness (kips/in)	Difference (kips/in)
9	28 (0.0149in.)	None	2.8	3.5	0.7
		24	19.6	22.0	2.4
		12	27.0	31.8	4.8
		8	31.8	38.7	6.9
	29 (0.0135in.)	None	2.8	3.5	0.7
		24	18.1	20.7	2.6
		12	24.7	29.7	5.0
		8	28.8	36.0	7.2
	30 (0.0120in.)	None	2.8	3.5	0.7
		24	16.4	19.2	2.8
		12	22.0	27.3	5.3
		8	25.5	32.8	7.3
12	26 (0.0179in.)	None	2.4	3.1	0.7
		24	22.4	24.3	1.9
		12	32.0	36.0	4.0
		8	38.4	44.5	6.1
	28 (0.0149in.)	None	2.4	3.1	0.7
		24	19.6	21.7	2.1
		12	27.3	31.7	4.4
		8	32.4	38.8	6.4
	29 (0.0135in.)	None	2.4	3.1	0.7
		24	18.1	20.4	2.3
		12	24.9	29.6	4.7
		8	29.3	36.0	6.7

Table 3 shows that the in-plane stiffness modulus for metal cladding, G_{MCA}, varied i between 2.4kips/in and 44.4kips/in. In the AED method, the in-plane stiffness modulus for metal cladding, G_{MCA}, is set as a variable. The stiffness of roof diaphragm and stiffness of endwall can be calculated in terms of G_{MCA}.

3.4 Stiffness of roof diaphragm

The stiffness of roof diaphragm, C_h, is calculated in terms of the in-plane stiffness modulus for metal cladding, G_{MCA}, as

$$C_h = \sum_{i=1}^{n} \frac{cos\theta_i}{\frac{a}{b*G_{MCA,i}} + \frac{2}{K_{R,i}}} \quad (2)$$

where,

θ_i = slope of diaphragm i from the horizontal

a = frame spacing

b = diaphragm length

$G_{MCA,i}$ = in-plane stiffness modulus for metal cladding of diaphragm i

$K_{R,i}$ = total stiffness of all the rafter-purlin and rafter-blocking connections for diaphragm i

$$K_R = (num)_p * K_p + (num)_{sb} * K_{sb} \quad (3)$$

where,

$(num)_p$ = the number of the purlins attached to the rafter

K_p = the stiffness of one rafter-purlin connection. See Table 1.

$(num)_{sb}$ = the number of shear blocks attached to rafter

K_{sb} = the stiffness of one shear block connection. See Table 1.

3.5 Stiffness of endwall

The end wall stiffness, k_e, can be calculated in terms of the in-plane stiffness modulus for metal cladding, G_{MCA}, as

$$k_e = \frac{\frac{a}{b}}{\frac{a}{b*G_{MCA}} + \frac{2}{K_g}} (cos\theta) \left(\frac{b_h}{a}\right) \quad (4)$$

where,

a = height of the end wall

b = post spacing

G_{MCA} = in-plane stiffness modulus for metal cladding

K_g = total stiffness of all the girt-to-post connections

Θ = slope from the vertical of wall diaphragm, usually equal to 0 degree

b_h = building width

Currently, there is no test data for the stiffness of girt-to-post connection, K_g. Aguilera (2014) assumed the stiffness of girt-to-post connection to be equal to 10kips/in. The ratio of predicted to test results was 0.81 with a coefficient of variation of 39% and the stiffness value is under predicted for most cases (Aguilera, 2014).

3.6 Diaphragm resistance force modifier (mD)

Diaphragm resistance force modifier (mD) is a reduction factor to calculate diaphragm resistance force to sidesway. (mD) ranges from 0 to 1. As (mD) approaches zero, more loads are carried by the frames. As (mD) approaches 1.0, more loads are carried by the roof diaphragm.

The diaphragm resistance force modifier (mD) can be calculated, if the stiffness of the roof diaphragm, the stiffness of the endwall and the frame stiffness are known. A derivation for (mD) values for 5-frame rectangular building is shown in Appendix A and the equation for (mD) can be express as:

$$\begin{pmatrix}(\mathrm{mD})_2\\(\mathrm{mD})_3\end{pmatrix} = (1-\frac{r'}{2})\begin{pmatrix} r+r'+1 & \frac{r}{2}+\frac{r'}{2} \\ r+r' & r+\frac{r'}{2}+1 \end{pmatrix}^{-1} \quad (5)$$

where,

r = k/C_h = the ratio of frame stiffness to stiffness of roof diaphragm

r' = k/k_e = the ratio of frame stiffness to end wall stiffness

Note that C_h and k_e are functions of G_{MCA}. Therefore, (mD) is a function of G_{MCA}.

3.7 Maximum horizontal eave deflection, Δ_{max}

The maximum horizontal eave deflection, Δ_{max}, is defined as the horizontal eave deflection at the critical frame (typically the middle frame) for a post-frame building. The maximum horizontal eave deflection, $\Delta_{max,}$ can be calculated by using the force resisted by the critical frame divided by its stiffness, k. The force resisted by the critical frame is calculated as

$$\Delta_{\max} = \frac{R-(\mathrm{mD})\mathrm{R}}{k} \quad (6)$$

where,

(mD) = (mD) value for the critical frame (typically the middle frame)

The next chapter will illustrate by an example how to use the equations to establish the relationship between stiffness of roof diaphragm and maximum horizontal eave deflection as well as the stiffness of endwall and maximum horizontal eave deflection. The stiffness of roof diaphragm and the stiffness of endwall can be calculated directly by defining the maximum horizontal eave deflection.

CHAPTER 4: EXAMPLE OF THE ALLOWABLE EAVE DEFLECTION METHOD

An example using the Allowable Eave Deflection method is presented in this chapter. The building specifications and wind loads are given below.

Building Specifications:

Building length (along ridge), L: 60ft

Building width (truss length), W: 36ft

Height to the eave, H_p: 12ft

Post & truss spacing, s: 10ft o.c.

Number of frames (including end walls): 7

Roof slope: 4:12

Post grade & lumber species: No.2 S. Pine

Post size: 6-by 6-in

Roof snow load: 30psf

Roof dead load: 5psf

Ceiling: No

Wind Loads:

Wind speed: 80mph

Exposure category: B

Windward wall pressure, q_{ww}: 8.13psf

Leeward wall pressure, q_{lw}: -5.08psf

Windward roof pressure, q_{wr}: 3.05psf

Leeward roof pressure, q_{lr}: -7.12psf

Negative loads act away from the surface of the structure. Positive loads act toward the surface of the structure.

Assumptions:

(1) All posts are assumed to be fixed at the grade line and pin-connected to the truss;

(2) There are no special members connecting posts to the truss.

(3) Stiffness values of both endwall are the same.

(4) Stiffness values of the frames are the same.

(5) Stiffness values of the diaphragms of both slopes of the roof are the same.

(6) Eave loads for all interior frames are the same.

(7) Eave load for the exterior frame is equal to one-half that of the interior frame

Allowable Eave Deflection method

1) Frame stiffness, k

Frame stiffness is obtained using a plane-frame structural analysis computer program (MASTAN). A horizontal point force of 100lb, P, applied at the eave height of the frame results in a horizontal deflection at the eave, Δ, 0.5428in (Figure 15).

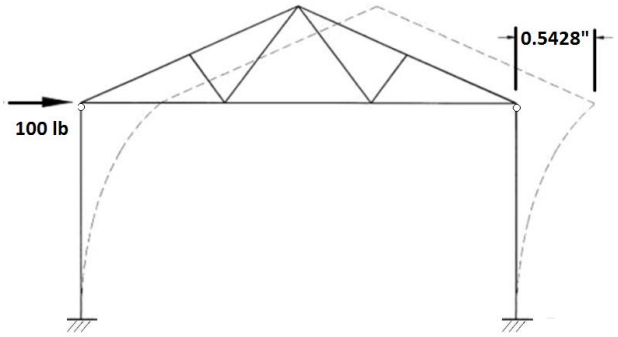

Figure 15 Structural analog for frame stiffness

$$\mathrm{k} = \frac{100\mathrm{lb}}{0.5428\mathrm{in}} = 184\ \mathrm{lb}/in$$

2) Eave loads, R

Eave load, R, is obtained by a plane-frame structural analysis (Figure 16).

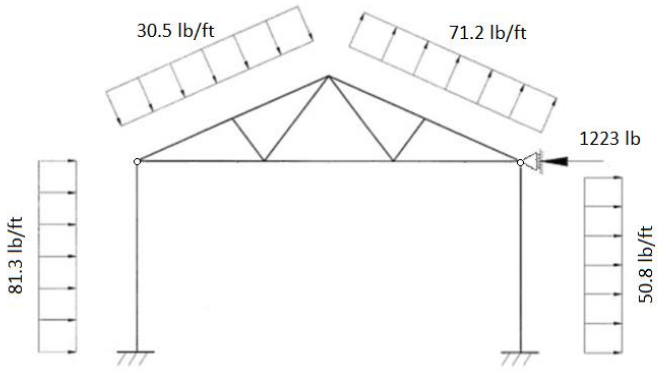

Figure 16 Structural analog for eave load

$$R = 1223\mathrm{lb}$$

3) Stiffness of roof diaphragm, C_h

The stiffness of the roof diaphragm, C_h, can be calculated in terms of G_{MCA} as:

$$C_h = \frac{2cos\theta}{\frac{a}{b * G_{MCA}} + \frac{2}{K_R}}$$

$$C_h = \frac{2\cos(18.43^\circ)}{\frac{10}{19G_{MCA}} + \frac{2}{20}} \approx \frac{361G_{MCA}}{19G_{MCA} + 100} \text{ (kips/in)}$$

where,

θ = 18.43 degrees = slope from the horizontal of diaphragm

a = 10ft = frame spacing shown in Figure 17

b = 19ft = diaphragm length shown in Figure 17

G_{MCA} = in-plane diaphragm stiffness modulus for metal cladding

K_R = 20 kips/in = stiffness of all the rafter- purlin and rafter-blocking connections (Leflar, 2008)

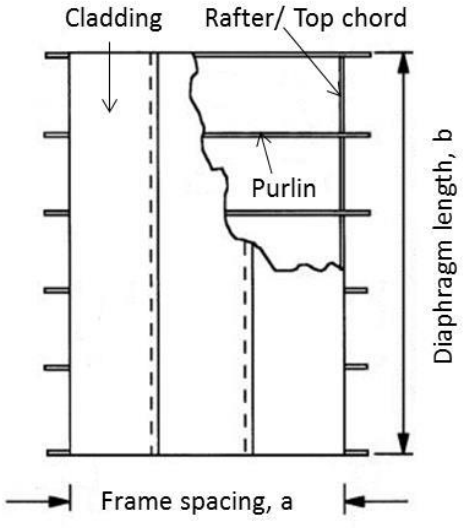

Figure 17 Sketch of roof diaphragm

4) End wall stiffness, k_e

End wall stiffness, k_e, can be calculate in terms of G_{MCA} as

$$k_e = \frac{\frac{a}{b}}{\frac{a}{b * G_{MCA}} + \frac{2}{K_g}} \left(\frac{b_h}{a}\right)$$

$$k_e = \frac{12/9}{\frac{12}{9G_i'} + \frac{2}{40}} \left(\frac{36}{12}\right) = \frac{240G_{MCA}}{3G_{MCA} + 80} \text{(kips/in)}$$

where,

a = 12ft = height of end wall shown in Figure 18

b = 9ft = end wall post spacing shown in Figure 18

G_{MCA} = in-plane stiffness modulus for metal cladding

K_g = 40kips/in = total stiffness of all the girt-to-post connections (Aguilera, 2014)

b_h = 36ft = building width

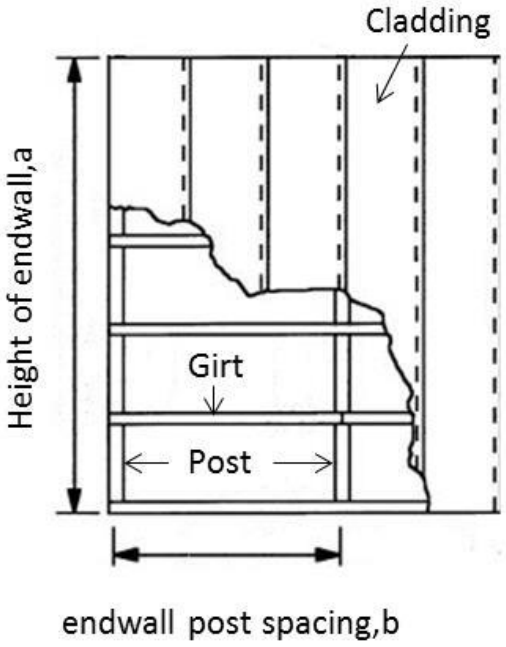

Figure 18 Sketch of endwall

5) Relationship between stiffness values (stiffness of roof diaphragm and stiffness of endwall) and maximum horizontal deflection

Based on the Monte Carlo Simulation, randomly select in-plane stiffness modulus for metal-cladding, G_{MCA}, from the range between 2.4 and 44.4 kips/in to calculate the simulation data including the stiffness of roof diaphragm, the stiffness of endwall and maximum horizontal deflection.

For example, in-plane stiffness modulus for metal-cladding, G_{MCA}, is equal to 7kips/in. Therefore, the stiffness of roof diaphragm and the stiffness of endwall can be calculated in terms of G_{MCA}

$$C_h = \frac{361G_{MCA}}{19G_{MCA} + 100} = 10.85(\text{kips/in})$$

$$k_e = \frac{240G_{MCA}}{3G_{MCA} + 80} = 16.63(\text{kips/in})$$

Calculation for mD value for 7-frame building based on equilibrium and compatibility yields (due to symmetry, only (mD) values for frame 2, 3 and 4 are shown)

$$\begin{bmatrix} (mD)_2 \\ (mD)_3 \\ (mD)_4 \end{bmatrix} = (1-\frac{r'}{2}) \bullet \begin{bmatrix} r+r'+1 & r+r' & \frac{r}{2}+\frac{r'}{2} \\ r+r' & 2\bullet r+r'+1 & r+\frac{r'}{2} \\ r+r' & 3\bullet r+r' & \frac{3\bullet r}{2}+\frac{r'}{2}+1 \end{bmatrix}^{-1} \bullet \begin{bmatrix} 1 \\ 1 \\ 1 \end{bmatrix} = \begin{bmatrix} 0.9294 \\ 0.9058 \\ 0.8980 \end{bmatrix}$$

where,

$(mD)_I$ = sidesway restraining force modifier for frame i

$r = k/C_h$ =184/10850 = 0.01696 = ratio of frame stiffness to stiffness of roof diaphragm

$r' = k/k_e$ =184/16630 = 0.01106 = ratio of frame stiffness to end wall stiffness

The critical frame for this building is the middle frame (frame 4). The (mD) value for frame 4 is equal to 0.8980. Therefore, the maximum horizontal eave deflection at the critical frame, Δ_{max} is calculated as

$$\Delta_{max} = \frac{R - (\mathrm{mD})\mathrm{R}}{k}$$

$$\Delta_{max} = \frac{1223 - (0.8980 * 1223)}{184} = 0.6680\mathrm{in}$$

where,

R = 1223lb = eave load

Q = (mD)*R = horizontal restraining force

k = 184lb/in = frame stiffness

One simulation data point is calculated from the above example when in-plane stiffness modulus for metal-cladding, G_{MCA}, is equal to 7kips/in. The AED method requires lots of simulation points to establish the relationship between stiffness values (stiffness of roof diaphragm and stiffness of endwall) and maximum horizontal deflection. An analysis result using 500 simulation points is shown in Figure 19.

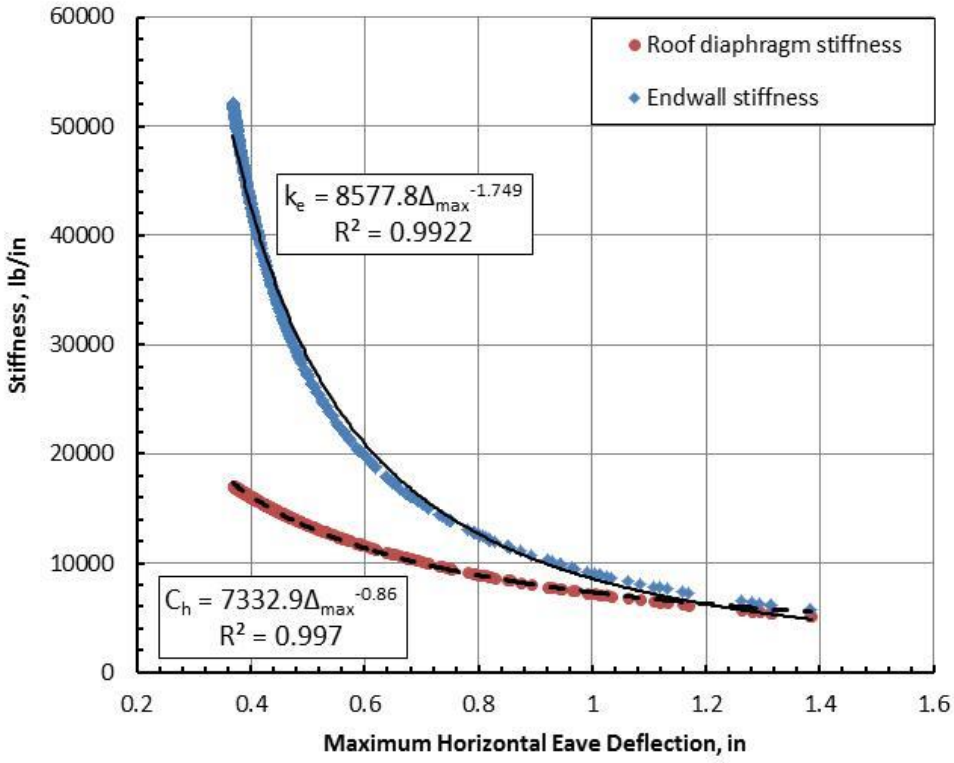

Figure 19 Relationship between stiffness values (stiffness of roof diaphragm and stiffness of endwall) and maximum horizontal deflection (500 simulation points)

CHAPTER 5: RESULTS AND DISCUSSION

This chapter contains four sections to discuss the Allowable Eave Deflection (AED) method. Section 5.1 describes how to select the function type to fit the relationship between stiffness values of metal-clad wood-frame diaphragm and horizontal maximum eave deflection. Section 5.2 presents the comparison between the AED method and the computer program DAFI to check calculation for the AED method. Section 5.3 shows a validation for the AED method using the results from the full-scale test by Gebremedhin et al. (1992). Section 5.4 shows sensitivity analysis for best-fit line between stiffness of metal-clad wood-frame diaphragm values and horizontal maximum eave deflection. Three variables are considered including post size, wind speed and the stiffness of rafter-purlin connections. Section 5.5 introduces the application for the AED method in post design.

5.1 Relationship between stiffness values versus maximum horizontal eave deflection curve

In this section, two functions are used to fit the relationship between stiffness of metal-clad wood-frame diaphragm and horizontal maximum eave deflection. R-square value is used to evaluate the relationship. The R-square is the coefficient of determination, which can be calculated directly by computer program Excel or MATLAB after selecting function type. R-square value can take on any value between 0 and 1, with a value closer to 1 indicating that a greater proportion of data points fit for the function.

(1) Exponential function

The result for the simulation data fit by exponential function is shown in Figure 20. The stiffness of roof diaphragm simulation data fits the exponential function well and R-square is

equal to 0.9795. However, the exponential function is not fitted for the stiffness of endwall as well as for the stiffness of roof diaphragm. The R-square value for end wall stiffness simulation data is equal to 0.9068.

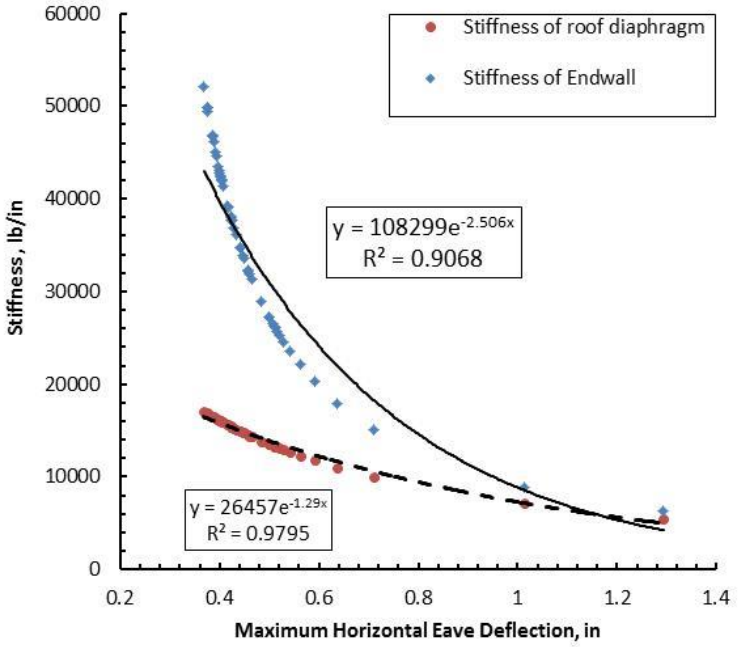

Figure 20 Exponential function analysis result for relationship between stiffness and maximum horizontal eave deflection

(2) Power function

The result for the simulation data using a power function is shown in Figure 21. The stiffness of roof diaphragm data and the stiffness of endwall data fit the power function very well. The R-square value for stiffness of the endwall data is equal to 0.989 and the R-square value for stiffness of the roof diaphragm data is 0.9958.

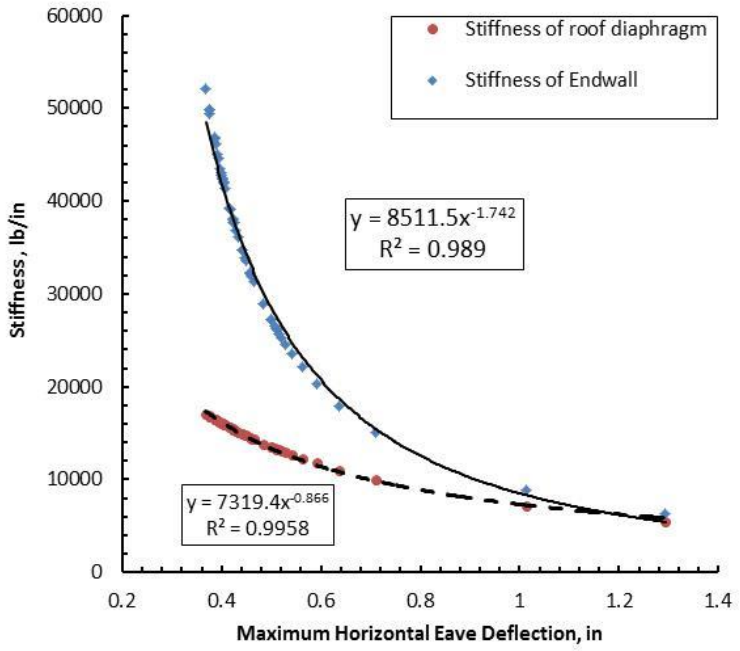

Figure 21 Power function analysis result for the relationship between stiffness and maximum horizontal eave deflection

Comparison between two functions, the power function is selected to be used as the best-fit line function to fit the relationship between stiffness of metal-clad wood-frame diaphragm and horizontal maximum eave deflection.

5.2 Check calculation for the AED method

The next 4 steps describe the method used to compare results from the AED method and the computer program DAFI to check calculation for the AED method: (1) Select several values (more than 10 values) from the range of maximum horizontal eave deflection; (2) Calculate stiffness of roof diaphragm and stiffness of endwall based on the equation of selected trend line type; (3) Set the stiffness values calculated by Step 2 as inputs for the computer program DAFI to determine horizontal eave deflection at the critical frame; (4) Compare the estimated eave deflections and calculated eave deflections from DAFI results.

The results of the comparison are shown in Table 4. The difference between the estimated eave deflections and calculated eave deflections from DAFI results is less than 2%. Therefore, this relationship can be used to calculate the stiffness of roof diaphragm and the stiffness of endwall.

Table 4 Comparison results between the AED method and computer program DAFI

a. Selected maximum horizontal eave deflection, in	b. Calculated stiffness of roof diaphragm, lb/in	c. Calculated stiffness of endwall, lb/in	d. Maximum horizontal eave deflection from DAFI, in	e. Difference between column a and column d
0.50	13309	28832	0.4986	0.3%
0.55	12262	24405	0.5487	0.2%
0.60	11378	20960	0.5991	0.1%
0.65	10621	18222	0.6498	0.0%
0.70	9965	16007	0.7007	-0.1%
0.75	9391	14187	0.7519	-0.3%
0.80	8884	12673	0.8033	-0.4%
0.85	8433	11398	0.8549	-0.6%
0.90	8028	10313	0.9067	-0.7%
0.95	7664	9383	0.9586	-0.9%
1.00	7333	8578	1.0106	-1.1%
1.05	7032	7876	1.0627	-1.2%

5.3 Validation for the AED method

In this section, the result of the full-scale test by Gebremedhin et al. (1992) is used to validate the AED method. The frame stiffness was equal to 69.6lb/in. The applied load at the eave height was equal to 815lb. The maximum horizontal eave deflection at the middle frame was equal to 0.98in. Gebremedhin et al. (1992) determined the stiffness of the roof diaphragm and the stiffness of the end wall by the process of iteration using the computer program DAFI. The stiffness of the roof diaphragm was equal to 18270lb/in. The stiffness of the endwall was equal to 7252lb/in.

The simulation result for the same building in the full-scale test using the AED method is shown in Figure 22. The stiffness of all purlin-rafter connection is assumed to be 70kips/in and the stiffness of girt-to-post connection is assumed to be 7kips/in. The selected maximum horizontal eave deflection is equal to 0.98in, which is the same as the result of the full-scale test. The calculated stiffness of roof diaphragm by the AED method is equal to 17360lb/in and the calculated stiffness of endwall by the AED method is equal to 7696lb/in.

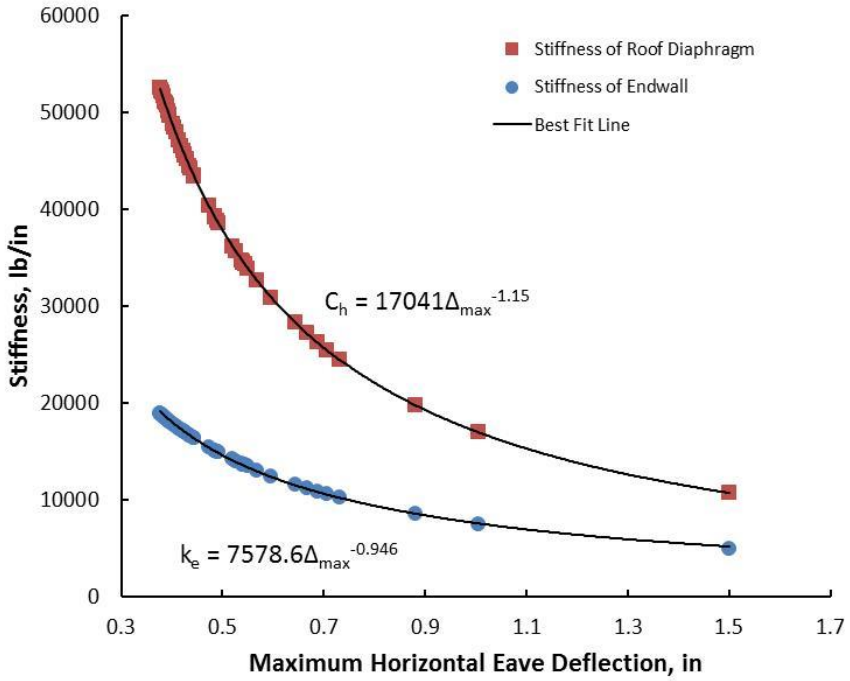

Figure 22 **Relationship between stiffness of roof diaphragm and maximum horizontal eave deflection for the full-scale test building by Gebremedhin et al. (1992)**

The difference between the stiffness of roof diaphragm determined by Gebremedhin et al. (1992) and the calculated stiffness of roof diaphragm by the AED method is less than 5%. The difference between the stiffness of endwall determined by Gebremedhin et al. (1992) and the calculated stiffness of endwall by the AED method is less than 6%.

5.4 Sensitivity Analysis

In this section, in order to analyze the effects of changing certain variables on the stiffness versus maximum horizontal eave deflection curve, a series of analyses were run to show the relative impact of each change. There are three variables discussed in this section:

(1) Post size

Three different post sizes (6-by-6in, 6-by-8 in, 8-by-8 in) are used to do sensitivity analysis. The results are shown in Figure 23 & 24.

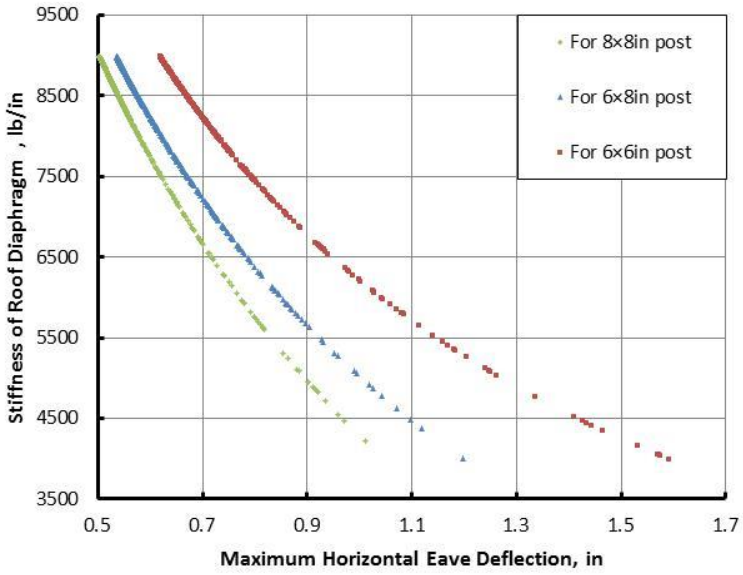

Figure 23 Sensitivity of post-size on stiffness of roof diaphragm

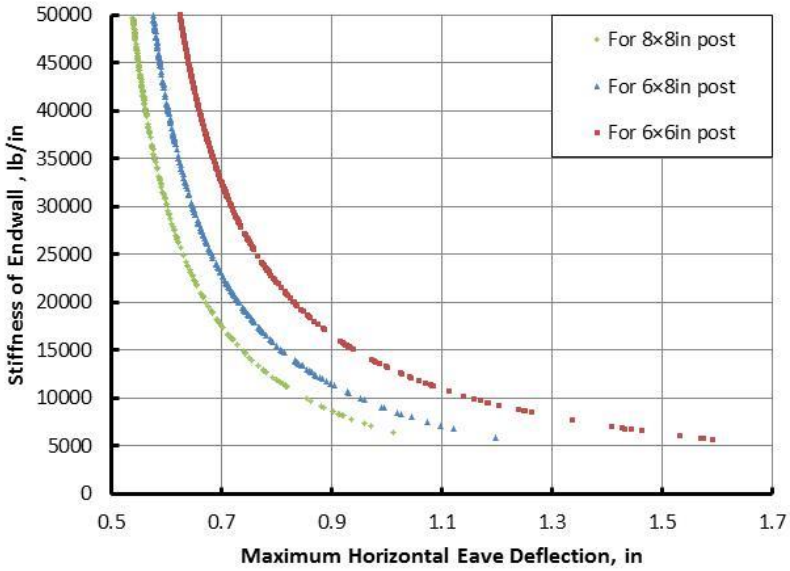

Figure 24 Sensitivity of post-size on stiffness of endwall

More results are given in Table 5 & 6. As the post-size increased from 6*6in to 8*8in, the stiffness of roof diaphragm decreased about 20% for the same horizontal eave deflection. The percent decrease of stiffness of roof diaphragm slightly increased (2%) when the maximum horizontal eave deflection increased from 0.7in to 0.9in. The stiffness of endwall decreased as the post-size increased from 6*6in to 8*8in. The percent decrease of stiffness of endwall was 24%, if the maximum horizontal eave deflection increased from 0.7in to 0.9in.

Table 5 Sensitivity of post-size on stiffness of roof diaphragm

Post size	Maximum Horizontal Eave Deflection, in		
	0.7	0.9	1.1
	Stiffness of roof diaphragm, lb/in	Stiffness of roof diaphragm, lb/in	Stiffness of roof diaphragm, lb/in
6×6 in	8233	6678	5529
6×8 in	7214	5626	4490
8×8 in	6654	4957	-

Table 6 Sensitivity of post-size on stiffness of endwall

Post size	Maximum Horizontal Eave Deflection, in		
	0.7	0.9	1.1
	Stiffness of endwall, lb/in	Stiffness of endwall, lb/in,	Stiffness of endwall, lb/in
6×6 in	32484	15882	10163
6×8 in	22701	11286	7154
8×8 in	17442	8626	-

2) Wind speed

Three different wind speeds are used to conduct sensitivity analysis (70mph, 80mph and 90mph). The sensitivity analysis results are shown in Figure 25 and 26.

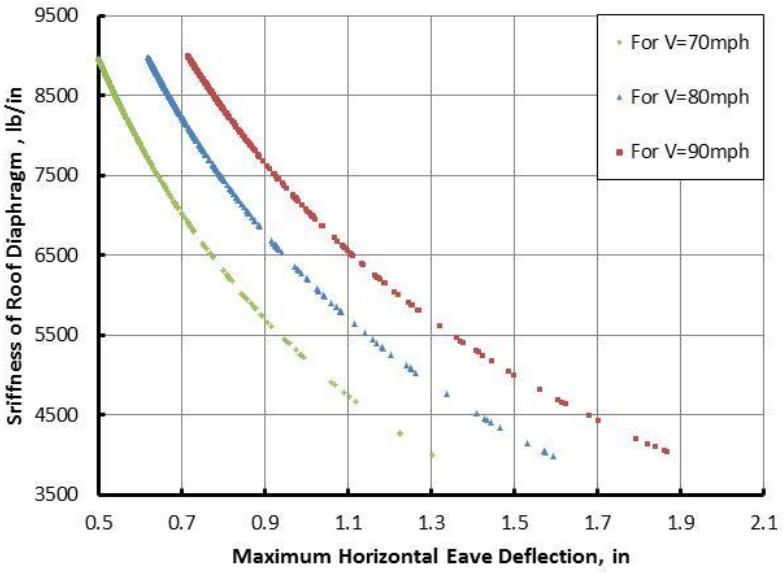

Figure 25 Sensitivity of wind speed on stiffness of roof diaphragm

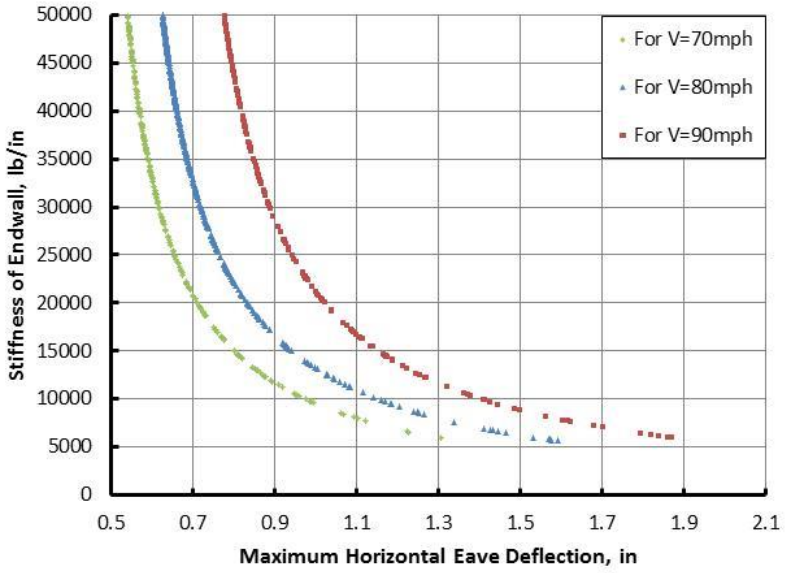

Figure 26 Sensitivity of wind speed on stiffness of endwall

More results are given in Table 7 & 8. As the wind speed increase from 70mph to 90mph, the stiffness of roof diaphragm increase when the maximum horizontal eave deflection is selected the same amount. The percent increase of stiffness of roof diaphragm slightly decrease when the maximum horizontal eave deflection increase. The stiffness of endwall increase as the wind speed increase from 70mph to 90mph. The percent increase of stiffness of endwall decrease, if the maximum horizontal eave deflection increase from 0.9in to 1.1in.

Table 7 Sensitivity of wind speed on stiffness of roof diaphragm

Wind speed	Maximum Horizontal Eave Deflection, in		
	0.7	0.9	1.1
	Stiffness of roof diaphragm, lb/in	Stiffness of roof diaphragm, lb/in	Stiffness of roof diaphragm, lb/in
70mph	7221	5664	4531
80mph	8233	6678	5529
90mph	-	7214	6153

Table 8 Sensitivity of wind speed on stiffness of endwall

Wind speed	Maximum Horizontal Eave Deflection, in		
	0.7	0.9	1.1
	Stiffness of endwall, lb/in	Stiffness of endwall, lb/in	Stiffness of endwall, lb/in
70mph	21048	12316	8538
80mph	32484	15882	10163
90mph	-	25394	14864

3) Stiffness of rafter-purlin connection, K_r

Three different stiffness of rafter-purlin connection are used to do sensitivity analysis. Because the database of stiffness of rafter-purlin connection is lacking, we use the minimum, average and maximum of the test data by Leflar (2008) to do sensitivity analysis. The minimum rafter-purlin connection is equal to 0.87kips/in. The average rafter-purlin connection is equal to 1.00kips/in. The maximum rafter-purlin connection is equal to 1.31kips/in. The sensitivity analysis results are shown in Figure 27 and 28.

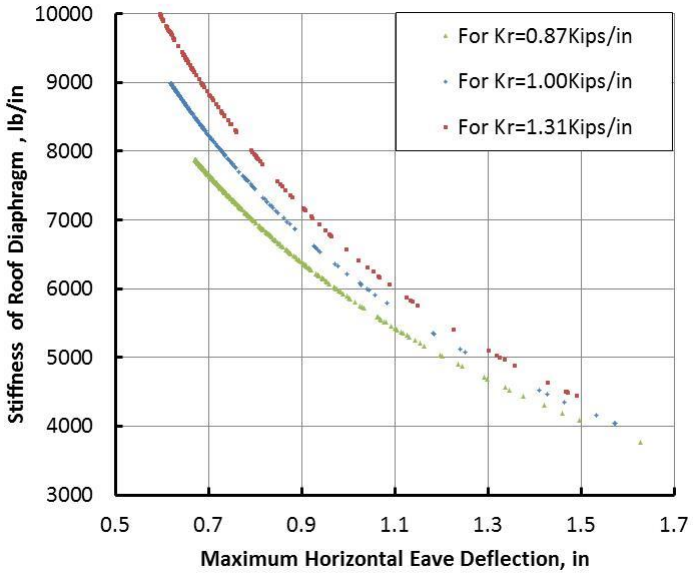

Figure 27 Sensitivity of stiffness of rafter-purlin connection on stiffness of roof diaphragm

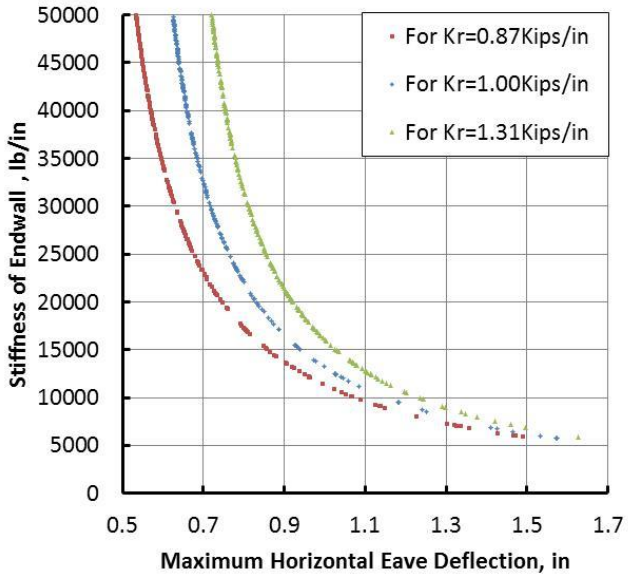

Figure 28 Sensitivity of stiffness of rafter-purlin connection on stiffness of endwall

More results are given in Table 9 & 10. As the purlin-rafter connection stiffness increase from 0.8 to 1.3kips/in, the stiffness of roof diaphragm increase when the maximum horizontal eave deflection is selected the same amount. The percent increase of stiffness of roof diaphragm decrease (about 4%) when the maximum horizontal eave deflection increase. However, as the purlin-rafter connection stiffness increase from 0.8 to 1.3kips/in, the stiffness of endwall decrease. The percent decrease of stiffness of roof diaphragm dramatically decrease (from 110% to11%), if the maximum horizontal eave deflection increase from 0.7in to 1.1in.

Table 9 Sensitivity of stiffness of rafter-purlin connection on stiffness of roof diaphragm

Purlin-rafter connection Stiffness, kips/in	Maximum Horizontal Eave Deflection, in		
	0.7	0.9	1.1
	Stiffness of roof diaphragm, lb/in	Stiffness of roof diaphragm, lb/in	Stiffness of roof diaphragm, lb/in
0.8	7651	6364	5318
1.0	8233	6678	5529
1.3	8814	7155	5862

Table 10 Sensitivity of stiffness of rafter-purlin connection on stiffness of endwall

Purlin-rafter connection Stiffness, kips/in	Maximum Horizontal Eave Deflection, in		
	0.7	0.9	1.1
	Stiffness of endwall, lb/in	Stiffness of endwall, lb/in	Stiffness of endwall, lb/in
0.8	58454	21183	12137
1.0	32484	15882	10163
1.3	22898	13582	9198

5.5 Application for the AED method in wood post design

In this section, a wood post design example is used to show how to apply the AED method in post design. In the design of post-frame building, there are three controlling design equations for checking wood post strength (NDS, 2005): shear, axial compression without bending, and axial compression with uniaxial bending. Shear and axial compression without bending can be easily checked. Post design equation for combined bending and compression is shown below (NDS, 2005):

$$CSI = \left(\frac{f_c}{F_c'}\right)^2 + \frac{f_b}{F_b'(1 - \frac{f_c}{F_{CE}})} \leq 1.0$$

where,

CSI = combined stress interaction

f_c = actual compressive stress = P/(bd) for rectangular members

F_c' = adjusted compression design value

f_b = actual bending stress (strong axis) = 6M/ (bd^2) for rectangular members

F_b' = adjusted bending design value (strong axis)

F_{CE} = critical buckling design values for compression (strong axis)

For a nominal 6-by-6in post, the geometrical properties are shown below:

b = d = 5.5in

A = 30.25in^2

S_x = 27.73in^3

I = 76.25 in^4

For No.2 Southern Pine timber, the tabulated compression and bending stresses and modulus of elasticity are:

F_b = 850psi = tabulated bending strength

F_c = 525psi = tabulated compression strength

E = 1200ksi = modulus of elasticity

Applicable adjustment factors are:

C_D = 1.60 = load duration factor, since the shortest duration load in the combination of loads

C_t = 1.00 = temperature factor, for using under normal temperature

C_M = 0.91 =wet service factor, for wood located near the soil surface

C_F = 1.00 = size factor, for nominal 6-by-6in No.2 Southern Pine

C_p = 1.00 = column stability factor, at the base of the post where support is provided in both directions

C_p = less than 1.00 between points of lateral support

C_L = 1.00 = beam stability factor, since post is square

Applied adjustment factors for design values:

$$\mathrm{F}'_c = F_c C_D C_M C_t C_P$$

$$\mathrm{F}'_c = 525(1.60)(0.91)(1.0)(1.0) = 765\ psi \text{ (at base)}$$

$$\mathrm{F}'_b = F_b C_D C_t C_F C_L$$

$$F'_b = 850(1.60)(1.0)(1.0)(1.0) = 1360psi$$

F_{CE} is a very large number if the effective buckling length, l_e, is assumed to be very small because of support at the base. As a result, the ratio f_c/F_{CE} is assumed to be equal to zero (NFBA Post-Frame Building Design Manual, 1999).

The actual compression force, P, is equal to 3821lb by using the analysis computer program MASTAN. The actual compression stress, f_c, is equal to 3821/30.25 = 126psi.

Assuming the CSI equal to 1 in order to find the critical horizontal eave deflection, the equation can be expressed as

$$CSI = \left(\frac{126}{765}\right)^2 + \frac{f_b}{1360} = 1$$

The critical bending stress and bending moment is calculated:

$$f_b = 1323psi$$

$$M_{max} = 1323psi * 27.73in^3 = 36690lb - in$$

The maximum bending moment can be also calculated by superposition (Figure 29) as

$$M_{max} = \frac{wH_p{}^2}{8} + \frac{3EI\Delta_{crit}}{H_p{}^2}$$

$$36690 = \frac{(81.3/12)(144)^2}{8} + \frac{3(1{,}200{,}000)(76.26)\Delta_{crit}}{(144)^2}$$

$$\Delta_{crit} = 1.4448in$$

where,

H_p = height of post to the eave

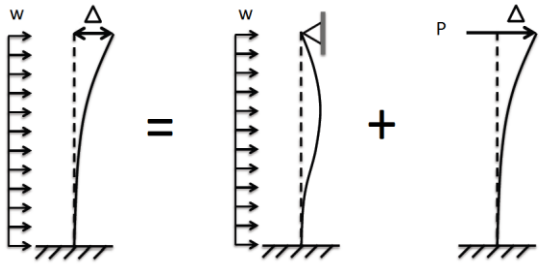

Figure 29 Analog to calculate bending moment

Besides, the International Building Code (IBC, 2009) specifies that the deflection limitation should be less than 144/120 =1.2in. Therefore, the minimum deflection limitation for 6-by-6in post in this example is 1.2in. Figure 30 shows the combination of the AED method and post design results. From Figure 30, we can see that if the maximum horizontal eave deflection for this particular building in the example is less than 1.2 in, there is no need to check the condition of axial compression with uniaxial bending.

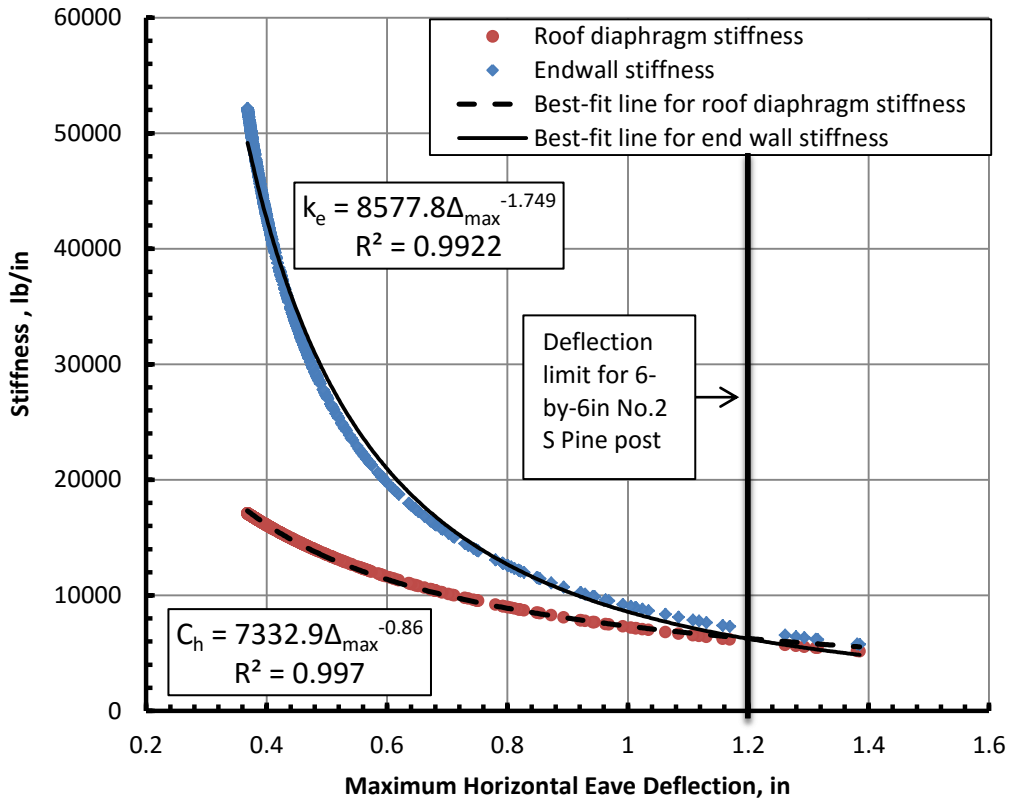

Figure 30 Application for the AED method in post design

CHAPTER 6: SUMMARY

This thesis presents an alternative method to design post-frame buildings without testing the whole metal-clad wood-frame (MCWF) diaphragm. The procedure is called Allowable Eave Deflection (AED) method. The AED method is an extension of the current work on the modified MCA procedure. The AED method utilizes the modified MCA procedure to establish the relationship between the stiffness of MCWF diaphragm and the horizontal eave deflection. The stiffness of MCWF diaphragm can be obtained by the defined maximum horizontal eave deflection.

Two functions are used to analyze the relationship between the stiffness of MCWF diaphragm and horizontal eave deflection. The power function is recommended to use as the best-fit line to fit the relationship.

The AED method was validated using the result of the full-scale test by Gebremedhin et al. (1992). The results show that the difference between the stiffness of roof diaphragm determined by Gebremedhin et al. (1992) and the calculated stiffness of roof diaphragm by the AED method is less than 5% and the difference between the stiffness of endwall determined by Gebremedhin et al. (1992) and the calculated stiffness of endwall by the AED method is less than 6%.

Sensitivity analysis was conducted to determine the level of influence of three variables (post size, wind speed and stiffness of purlin-rafter connection) on the relationship between the stiffness of MCWF diaphragm and maximum eave deflection. Among the three variables, the

database for stiffness of purlin-rafter connection is still lacking in literature. Further research is required to test the purlin-rafter connection for the stiffness.

REFERENCES

Aguilera, D., D. A. Bender and G. A. Anderson. 2014. Update on Diaphragm Design Value Determination Using the Modified MCA Procedure.

Aguilera, D. 2014.Development of Strength and Stiffness Design Values for Metal-clad, Wood-Framed Diaphragms. M.S. thesis, Department of Civil and Environmental Engineering, Washington State University.

American Forest & Paper Association, Inc., National Design Specification for Wood Construction, 2008 edition, Washington, DC.

Anderson, G. A., D. S. Bundy and N. F. Meador. 1989. The Force Distribution Method: Procedure and Application to The Analysis of Buildings with Diaphragm action. Transactions of the ASAE 32(5):1791-1796.

ASAE. 2012. ANSI/ASAE EP-484.2.Diaphragm Design of Metal-Clad, Post-Frame Rectangular Buildings. ABASE Standards, Engineering Practices, and Data St. Joseph, Mich.:American Society of Agricultural and Biological Engineers.

ASAE. 2014. ASAE Standard EP-558. Load Tests for Metal-Clad Wood-Frame Diaphragms. ASABE Standards, Engineering Practices, and Data, American Society of Agricultural and Biological Engineers, St. Joseph, MI.

Anderson, G.A. 2011. Modification of the MCA Procedure of Strength and Stiffness of Diaphragms used in Post-Frame Construction. Frame Building News (June):22-25.

Bohnhoff, D. 1992. Expanding Diaphragm Analyses for Post-Frame Buildings. Applied Engineering in Agriculture 8(4):509-517.

CMEC. 2013. Development of Design Data for Metal-clad, Wood-Framed Diaphragms. CMEC Technical Report 12-004. Composite Materials & Engineering Center (CMEC), Washington State University, Pullman, WA. www.cmec.wsu.edu.

Gebremedhin, K. G., E. L. Bahler and S.R.Humphreys.1986. A Modified Approach to Post-Frame Design Using Diaphragm Theory. Transactions of ASAE 29(5):1364-1372.

Gebremedhin, K. G. 1987a. SOLVER: An Interactive Structures Analyzer for Microcomputers. Northeast Regional Agricultural Engineering Service. Cornell University.

Gebremedhin, K. G. 1987b. METCLAD: Diaphragm Design of Metal-Clad Post-Frame Buildings using Microcomputers. Northeast Regional Agricultural Engineering Service. Cornell University.

Gebremedhin, K. G., J. A. Bartsch and M. C. Jorgensen. 1992. Predicting Roof Diaphragm and Stiffness of endwall From Full- Scale Test Results of A Metal-Clad, Post-Frame Building. Transactions of the ASAE 01/1992; 35(3):977-985.

Hoagland, R. C. and D. S. Bundy. 1983. Post-Frame Design Using Diaphragm Theory. Transactions of the ASAE 26(5):1499-1503.

Hoagland, R. C. and D. S. Bundy. 1983. Strength and Stiffness of screw-fastened roof panels for pole buildings. Transactions of the ASAE 26(2):512-515.

Leflar, J. A. 2008. A Mathematical Model of Metal-clad Wood-Frame Shear Diaphragms. M.S. thesis, Department of Civil and Environmental Engineering, Colorado State Univeristy.

Lukens, A.D., & Bundy. D.S. 1987. Strength and Stiffness of Post-Frame Building Roof Panels. ASAE Paper No. 874056. ASABE, St. Joseph, MI.

Luttrell, L.D. and J.A.Mattingly. 2004. A Primer on Diaphragm Design. Metal Construction Association. Glenview, IL.

Mill, D. P. 2012. Simplified Lateral Design of Post-Frame Buildings – Comparison of Design Methodologies and Underlying Assumption. M.S. thesis, Department of Civil and Environmental Engineering, Washington State University.

Niu, K. T., and Gebremedhin, K. G. 1997a. Evaluation of Interaction of Wood Framing Metal-Cladding in Roof Diaphragms. Transactions of the ASAE 40(2):465-476.

Niu, K. T., and Gebremedhin, K. G. 1997b. Three-Dimension Building Stiffness Model for Post-Frame Buildings. Transactions of the ASAE 40(3):795-801.

National Frame Building Association. 2015. Post-Frame Building Design Manual. National Frame Building Association, IL.

Ross, L.A., D.A. Bender and D.M.Carradine. 2009. Strength and Stiffness of Post-Frame Shear Wall with Wood Plastic Composite Skirtboards. Frame Builder News, November 2009.

APPENDIX A: DERIVATION OF DIAPHRAGM RESISTANCE FORCE MODIFIER

As an example, a typical rectangular post-frame building of five frames is shown in Figure A1. Horizontal eave loads and the corresponding horizontal eave deflections for the building are shown in Figure A2.

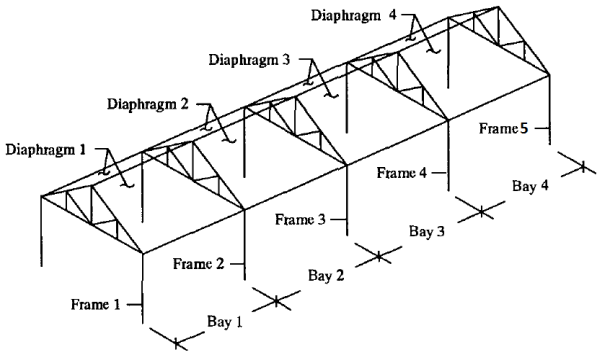

Figure A1. Post-frame building of 5 frames

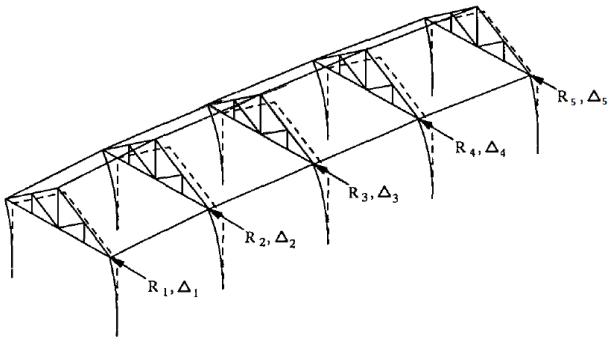

Figure A2. Horizontal eave loads and eave deflection

Assumption:

(1) Spacing between each frame is constant.

(2) Stiffness values of the frames are the same.

(3) Stiffness values of the diaphragms of both slopes of the roof are the same.

(4) Eave loads for all interior frames are the same.

(5) Eave load for the exterior frame is equal to one-half that of the interior frame

Derivation:

k = frame stiffness,

C_h = horizontal shear stiffness of roof diaphragm,

$r = k/C_h$ = ratio of frame stiffness to horizontal shear stiffness of roof diaphragm,

k_{ew} = end wall stiffness,

$r' = k/k_{ew}$ = ratio of frame stiffness to end wall stiffness,

R = eave Load,

$P_{f,i}$ = force resisted by frame i,

Δ_i = horizontal eave deflection on frame i,

$P_{r,i}$ = force resisted by roof at frame i,

mD_i = diaphragm resistance force modifier for frame i.

For frame 1 (end wall):

Calculate the force resisted by frame 1 (end wall):

$$P_{f,1} = k_{ew} * \Delta_1 \quad \text{(A1)}$$

Calculate the force resisted by roof diaphragm 1 at frame 1 (end wall):

$$P_{r,1} = C_h * (\Delta_1 - \Delta_2) \quad \text{(A2)}$$

The eave load is equal to the sum of the force resisted by frame and roof:

$$R/2 = P_{f,1} + P_{r,1} \quad \text{(A3)}$$

Combining equations (A1), (A2), and (A3):

$$(k_{ew} + C_h) * \Delta_1 = R/2 + C_h * \Delta_2 \quad \text{(A4)}$$

For Frame 2:

Calculate the force resisted by frame 2:

$$P_{f,2} = k * \Delta_2 \quad \text{(A5)}$$

Calculate the force resisted by roof diaphragm at frame 2:

$$P_{r,2} = C_h * ((\Delta_2 - \Delta_1) - (\Delta_3 - \Delta_2)) \quad \text{(A6)}$$

The eave load is equal to the sum of force resisted by frame and roof diaphragm:

$$R = P_{f,2} + P_{r,2} \quad \text{(A7)}$$

Combining equations (A5) and (A7):

$$R = \mathrm{k} * \Delta_2 + P_{r,2} \quad \text{(A8)}$$

For frame 3:

Calculate the force resisted by frame 3:

$$P_{f,3} = k * \Delta_3 \quad \text{(A9)}$$

Calculate the force resisted by roof diaphragm at frame 3:

$$P_{r,3} = 2 * C_h * (\Delta_3 - \Delta_2) \quad \text{(A10)}$$

The eave load is calculated by summing the force resisted by frame and roof diaphragm:

$$R = P_{f,3} + P_{r,3} \quad \text{(A11)}$$

Combining equations (A9) and (A11):

$$R = \mathrm{k} * \Delta_3 + P_{r,3} \quad \text{(A12)}$$

Arranging equations (A6) and (A10):

$$\Delta_2 = P_{r,2}/C_h + P_{r,3}/(2 * C_h) + \Delta_1 \quad \text{(A13)}$$

$$\Delta_3 = P_{r,2}/C_h + P_{r,3}/C_h + \Delta_1 \quad \text{(A14)}$$

Substituting equation (A13) into equations (A4):

$$\mathrm{k} * \Delta_1 = \frac{r'}{2} * R + r' * P_{r,2} + \frac{r'}{2} * P_{r,3} \quad \text{(A15)}$$

Substituting equations (A13) and (A14) into equations (A8) and (A12):

$$R = (\mathrm{r} + 1) * P_{r,2} + \frac{r}{2} * P_{r,3} + \mathrm{k} * \Delta_1 \quad \text{(A16)}$$

$$R = r * P_{r,2} + (\mathrm{r} + 1) * P_{r,3} + \mathrm{k} * \Delta_1 \quad \text{(A17)}$$

Substituting equation (A15) into equations (A16) and (A17) and arranging into a matrix form:

$$\begin{pmatrix} r + r' + 1 & \frac{r}{2} + \frac{r'}{2} \\ r + r' & r + \frac{r'}{2} + 1 \end{pmatrix} \begin{pmatrix} P_{r,2} \\ P_{r,3} \end{pmatrix} = (1 - \frac{r'}{2}) \begin{pmatrix} R \\ R \end{pmatrix} \quad \text{(A18)}$$

The diaphragm resistance modifier (mD_i) for frame i:

$$(\mathrm{mD})_2 = P_{r,2}/R \quad \text{(A19)}$$

$$(\mathrm{mD})_3 = P_{r,3}/R \quad \text{(A20)}$$

Substituting equations (A19) and (A20) into equation (A18):

$$\begin{pmatrix} (\mathrm{mD})_2 \\ (\mathrm{mD})_3 \end{pmatrix} = (1 - \frac{r'}{2}) \begin{pmatrix} r + r' + 1 & \frac{r}{2} + \frac{r'}{2} \\ r + r' & r + \frac{r'}{2} + 1 \end{pmatrix}^{-1} \quad \text{(A21)}$$

APPENDIX B: CONNECTIONS FOR POST-FRAME BUILDINGS

(1) Post-truss connections

One of the post-truss connections is shown in Figure B1. The advantage of this connection is the fasteners used to attach the truss to the post can be placed in double shear. This post-truss connection may be a semi-rigid connection but should be treated as a pin connection unless joint stiffness is known.

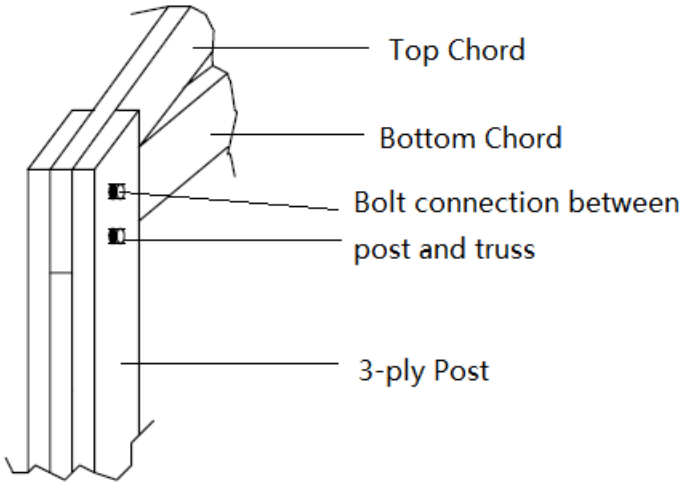

Figure B1 Sketch of post-truss connection

(2) Foundation

The preservative-treated wood post foundation is the most common used for the foundation in post-frame buildings (Figure B2).There are three common backfill materials: concrete, controlled low-strength material (CLSM) and excavated soil (NFBA Post-Frame Building Design Manual, 2015). The bottom end of the post can be assumed fix, if embed in concrete.

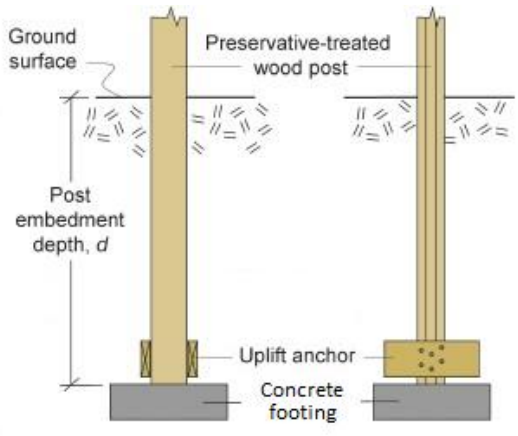

Figure B2 Preservative-treated wood post foundation (NFBA Post-Frame Building Design Manual, 2015)